

Studying Double Charm Decays of $B_{u,d}$ and B_s Mesons in the MSSM with R-parity Violation

C. S. Kim^{1*}, Ru-Min Wang^{1†} and Ya-Dong Yang^{2‡}

¹ *Department of Physics and IPAP, Yonsei University, Seoul 120-479, Korea*

² *Institute of Particle Physics, Huazhong Normal University, Wuhan 430070, P.R.China*

December 12, 2018

Abstract

Motivated by the possible large direct CP asymmetry of $\bar{B}_d^0 \rightarrow D^+ D^-$ decay measured by Belle collaboration, we investigate double charm $B_{u,d}$ and B_s decays in the minimal supersymmetric standard model with R-parity violation. We derive the bounds on relevant R-parity violating couplings from the current experimental data, which show quite consistent measurements among relative collaborations. Using the constrained parameter spaces, we explore R-parity violating effects on other observables in these decays, which have not been measured or have not been well measured yet. We find that the R-parity violating effects on the mixing-induced CP asymmetries of $\bar{B}_d^0 \rightarrow D^{(*)+} D^{(*)-}$ and $\bar{B}_s^0 \rightarrow D_s^{(*)+} D_s^{(*)-}$ decays could be very large, nevertheless the R-parity violating effects on the direct CP asymmetries could not be large enough to explain the large direct CP violation of $\bar{B}_d^0 \rightarrow D^+ D^-$ from Belle. Our results could be used to probe R-parity violating effects and will correlate with searches for direct R-parity violating signals in future experiments.

PACS Numbers: 12.60.Jv, 12.15.Ji, 13.25.Hw, 14.40.Lb

*E-mail: cskim@yonsei.ac.kr

†E-mail: ruminwang@cskim.yonsei.ac.kr

‡E-mail: yangyd@iopp.cnu.edu.cn

1 Introduction

Double charm decays of $B_{u,d}$ and B_s provide us with a rich field to study CP violation and final-state interactions as well as to extract information of Cabibbo-Kobayashi-Maskawa (CKM) elements. CP asymmetries (CPAs) in these decays play important roles in testing the Standard Model (SM) as well as exploring new physics (NP) [1, 2].

Double charm decays, $\bar{B}_d^0 \rightarrow D^{(*)+} D^{(*)-}$, $B_u^- \rightarrow D^{(*)0} D^{(*)-}$ and $\bar{B}_s^0 \rightarrow D_s^{(*)+} D^{(*)-}$, are dominated by color-allowed tree $b \rightarrow c\bar{c}d$ transition, but involve small penguin pollution from $b \rightarrow u\bar{u}d$ transition carrying a different weak phase. The latter contributions lead to direct CPAs, which are very small (about the order of 10^{-2}) in the SM. If penguin corrections are neglected, the SM predictions for the direct CPAs would be zero. It is interesting to note that both BABAR and Belle have measured the direct CPA in $B_d^0 \rightarrow D^+ D^-$ decay

$$\mathcal{C}(B_d^0, \bar{B}_d^0 \rightarrow D^+ D^-) = \begin{cases} -0.91 \pm 0.23 \pm 0.06 & \text{(Belle [3])}, \\ -0.07 \pm 0.23 \pm 0.03 & \text{(BABAR [4])}, \end{cases} \quad (1)$$

respectively. One would find the difference between the two measurements is

$$\Delta\mathcal{C} = 0.84 \pm 0.32, \quad (2)$$

i.e., the difference is as large as 2.7σ . So far, such a large direct CPA has not been observed in the other measurements of $\bar{B}_d^0 \rightarrow D^{(*)+} D^{(*)-}$, $B_u^- \rightarrow D^{(*)0} D^{(*)-}$ and $\bar{B}_s^0 \rightarrow D_s^{(*)+} D^{(*)-}$ decays [4, 5, 6, 7, 8, 9, 10, 11], which involve the same quark level weak decays. If the large CP violation in $\bar{B}_d^0 \rightarrow D^+ D^-$ from Belle is true, it would establish the presence of NP. At present one cannot conclude the presence of NP in those decays. Equivalently one also cannot take the CPAs are in agreement with the SM expectations. Recently the large direct CPA in $\bar{B}_d^0 \rightarrow D^+ D^-$ has been investigated with possible NP scenarios, such as unparticle interaction [12] and the NP effects in electroweak penguin sector [13, 14], and so on.

In this paper, we would like to investigate $B_{u,d}$ and B_s double charm decays systematically in the minimal supersymmetric standard model (MSSM) [15, 16] with R-parity violation [17, 18]. In the literature, the possible appearance of the R-parity violating (RPV) couplings [17, 18], which violate the lepton and/or baryon number conservations, has gained full attention in searching for supersymmetry [19, 20]. The effects of supersymmetry with R-parity violation in B meson decays have been extensively investigated, for instance in Refs. [21, 22, 23, 24]. In our work, twenty-four double charm decays $\bar{B}_d^0 \rightarrow D^{(*)+} D_{(s)}^{(*)-}$, $\bar{B}_u^- \rightarrow D^{(*)0} D_{(s)}^{(*)-}$ and $\bar{B}_s^0 \rightarrow$

$D_s^{(*)+} D_s^{(*)-}$ are studied in the RPV MSSM. For simplicity we employ naive factorization [25] for the hadronic dynamics, which is expected to be reliable for the color-allowed amplitudes, which are dominant contributions in those double charm decays.

The color-allowed tree level dominated decays of $b \rightarrow c\bar{c}d$, *i.e.* $\bar{B}_d^0 \rightarrow D^{(*)+} D^{(*)-}$, $B_u^- \rightarrow D^{(*)0} D^{(*)-}$ and $\bar{B}_s^0 \rightarrow D_s^{(*)+} D_s^{(*)-}$, involve the same set of RPV coupling constants. For these processes, besides the CPA in $\bar{B}_d^0 \rightarrow D^+ D^-$, a few other observables in $B_{u,d} \rightarrow D^{(*)} D^{(*)}$ have been already measured by BABAR and Belle collaborations [3, 4, 5, 6, 7, 8, 9, 10, 11, 26]. To derive constraints on the relevant RPV couplings, we will choose a set of data from the aforementioned measurements which have quite high consistency between the measurements of BABAR and Belle. Then, using the constrained RPV coupling parameter spaces, we predict the RPV effects on the other observables in $\bar{B}_d^0 \rightarrow D^{(*)+} D^{(*)-}$, $B_u^- \rightarrow D^{(*)0} D^{(*)-}$ and $\bar{B}_s^0 \rightarrow D_s^{(*)+} D_s^{(*)-}$ decays, whose measurements from BABAR and Belle are not compatible within 2σ error range, and/or which have not been measured yet. One of our goals is to see how large the direct CPA of $\bar{B}_d^0 \rightarrow D^+ D^-$ can be within the constrained parameter spaces. We find that the lower limit of $\mathcal{C}(B_d^0, \bar{B}_d^0 \rightarrow D^+ D^-)$ could be just slightly decreased by the RPV couplings, and the RPV effects on this quantity are not large enough to explain the large direct CP violation from Belle, although the mixing-induced CPAs of $\bar{B}_d^0 \rightarrow D^{(*)+} D^{(*)-}$ are very sensitive to the RPV couplings.

Decays $\bar{B}_d^0 \rightarrow D^{(*)+} D_s^{(*)-}$, $B_u^- \rightarrow D^{(*)0} D_s^{(*)-}$ and $\bar{B}_s^0 \rightarrow D_s^{(*)+} D_s^{(*)-}$ are governed by the $b \rightarrow c\bar{c}s$ transition at the quark level, and also involve the same set of RPV coupling constants. They have similar properties to $\bar{B}_d^0 \rightarrow D^{(*)+} D^{(*)-}$, $B_u^- \rightarrow D^{(*)0} D^{(*)-}$ and $\bar{B}_s^0 \rightarrow D_s^{(*)+} D_s^{(*)-}$ decays, nevertheless the penguin effects are less Cabibbo-suppressed. For these decays, most branching ratios and one longitudinal polarization have been measured [27, 28, 29, 30, 31, 32, 33, 34]. We will take the same strategy as the one for $b \rightarrow c\bar{c}d$ decays to constrain relevant RPV couplings and estimate RPV effects in these decays. We find that RPV couplings could significantly affect the CPAs of these decays, and could flip their signs.

Our paper is organized as follows: In Sec. 2, we briefly introduce the theoretical framework for the double charm $B_{u,d}$ and B_s decays in the RPV MSSM, and we tabulate all the theoretical input parameters. In Sec. 3, we deal with the numerical results and our discussions. At first, we give the SM predictions with full uncertainties of the input parameters. Then, we derive the constrained parameter spaces which satisfy all the experimental data with high consistency between different collaborations. Finally, we predict the RPV effects on other quantities, which

have not been measured or have not been well measured yet. Section 4 contains our summary.

2 Theoretical Framework

2.1 Decay amplitudes in the SM

In the SM, the low energy effective Hamiltonian for $\Delta B = 1$ transition at a scale μ is given by [35]

$$\mathcal{H}_{\text{eff}}^{\text{SM}} = \frac{G_F}{\sqrt{2}} \sum_{p=u,c} \lambda_p \left\{ C_1 Q_1^p + C_2 Q_2^p + \sum_{i=3}^{10} C_i Q_i + C_{7\gamma} Q_{7\gamma} + C_{8g} Q_{8g} \right\} + h.c., \quad (3)$$

here $\lambda_p = V_{pb}V_{pq}^*$ for $b \rightarrow q$ transition ($p \in \{u, c\}, q \in \{d, s\}$). The detailed definition of the effective Hamiltonian can be found in [35].

It is empirically observed that naive factorization [25] still works reasonably well in the color-allowed double charm $B_{u,d}$ and B_s decay processes. We will describe the $B \rightarrow D^{(*)} D_q^{(*)}$ decay amplitudes within the naive factorization approximation in this paper. Under the naive factorization approximation, the factorized matrix elements are given by

$$A_{[BD^{(*)}, D_q^{(*)}]} \equiv \langle D_q^{(*)} | \bar{q} \gamma^\mu (1 - \gamma_5) c | 0 \rangle \langle D^{(*)} | \bar{c} \gamma_\mu (1 - \gamma_5) b | B \rangle. \quad (4)$$

Decay constants and form factors [36, 37] are usually defined as

$$\langle D_q(p_{D_q}) | \bar{q} \gamma^\mu \gamma_5 c | 0 \rangle = -i f_{D_q} p_{D_q}^\mu, \quad (5)$$

$$\langle D_q^*(p_{D_q^*}) | \bar{q} \gamma^\mu c | 0 \rangle = f_{D_q^*} p_{D_q^*}^\mu, \quad (6)$$

$$\langle D(p_D) | \bar{c} \gamma_\mu b | B(p_B) \rangle = \left[(p_B + p_D)_\mu - \frac{m_B^2 - m_D^2}{q^2} q_\mu \right] F_1(q^2) + \frac{m_B^2 - m_D^2}{q^2} q_\mu F_0(q^2), \quad (7)$$

$$\langle D^*(p_{D^*}, \varepsilon^*) | \bar{c} \gamma_\mu b | B(p_B) \rangle = \frac{2V(q^2)}{m_B + m_{D^*}} \epsilon_{\mu\nu\alpha\beta} \varepsilon^{*\nu} p_B^\alpha p_{D^*}^\beta, \quad (8)$$

$$\begin{aligned} \langle D^*(p_{D^*}, \varepsilon^*) | \bar{c} \gamma_\mu \gamma_5 b | B(p_B) \rangle &= i \left[\varepsilon_\mu^* (m_B + m_{D^*}) A_1(q^2) - (p_B + p_{D^*})_\mu (\varepsilon^* \cdot p_B) \frac{A_2(q^2)}{m_B + m_{D^*}} \right] \\ &\quad - i q_\mu (\varepsilon^* \cdot p_B) \frac{2m_{D^*}}{q^2} [A_3(q^2) - A_0(q^2)], \end{aligned} \quad (9)$$

with $q = p_B - p_{D^{(*)}}$. Then we can express $A_{[BD^{(*)}, D_q^{(*)}]}$ in terms of decay constants and form

factors as follows

$$A_{[BD^{(*)}, D_q^{(*)}]} = \begin{cases} if_{D_q}(m_B^2 - m_D^2)F_0(m_{D_q}^2) & (DD_q), \\ 2f_{D_q^*}m_B|p_c|F_1(m_{D_q^*}^2) & (DD_q^*), \\ -2f_{D_q}m_B|p_c|A_0(m_{D_q}^2) & (D^*D_q), \\ -if_{D_q^*}m_{D_q^*} \left[(\varepsilon_{D^*}^* \cdot \varepsilon_{D_q^*}^*)(m_B + m_{D^*})A_1(m_{D_q^*}^2) \right. \\ \quad \left. - (\varepsilon_{D^*}^* \cdot p_{D_q^*})(\varepsilon_{D_q^*}^* \cdot p_{D^*}) \frac{2A_2(m_{D_q^*}^2)}{m_B + m_{D^*}} \right. \\ \quad \left. + i\epsilon_{\mu\nu\alpha\beta}\varepsilon_{D_q^*}^{*\mu}\varepsilon_{D^*}^{*\nu}p_{D_q^*}^\alpha p_{D^*}^\beta \frac{2V(m_{D_q^*}^2)}{m_B + m_{D^*}} \right] & (D^*D_q^*). \end{cases} \quad (10)$$

Decays $B \rightarrow D^{(*)} D_q^{(*)}$ may occur through both tree level and loop induced (penguin) quark diagrams, and the SM decay amplitudes within the naive factorization are given as

$$\mathcal{M}^{\text{SM}}(B \rightarrow D^{(*)} D_q^{(*)}) = \frac{G_F}{\sqrt{2}} \left(\lambda_c a_1^c + \sum_{p=u,c} \lambda_p [a_4^p + a_{10}^p + \xi(a_6^p + a_8^p)] \right) A_{[BD^{(*)}, D_q^{(*)}]}, \quad (11)$$

where the coefficients $a_i^p = (C_i + \frac{C_{i\pm 1}}{N_c}) + P_i^p$ with the upper (lower) sign applied when i is odd (even), and P_i^p account for penguin contractions. The factorization parameter ξ in Eq. (11) arises from the transformation of $(V - A)(V + A)$ currents into $(V - A)(V - A)$ ones for the penguin operators Q_5, \dots, Q_8 , and it depends on properties of the final-state mesons

$$\xi = \begin{cases} +\frac{2m_{D_q}^2}{(\bar{m}_c + \bar{m}_q)(\bar{m}_b - \bar{m}_c)} & (DD_q), \\ 0 & (DD_q^*), \\ -\frac{2m_{D_q}^2}{(\bar{m}_c + \bar{m}_q)(\bar{m}_b + \bar{m}_c)} & (D^*D_q), \\ 0 & (D^*D_q^*). \end{cases} \quad (12)$$

For the penguin contractions, we will consider not only QCD and electroweak penguin operator contributions but also contributions from the electromagnetic and chromomagnetic dipole operators. P_i^p are given as follows

$$\begin{aligned} P_1^c &= 0, \\ P_4^p &= \frac{\alpha_s}{9\pi} \left\{ C_1 \left[\frac{10}{9} - G_{D_q^{(*)}}(m_p) \right] - 2F_1 C_{8g}^{\text{eff}} \right\}, \\ P_6^p &= \frac{\alpha_s}{9\pi} \left\{ C_1 \left[\frac{10}{9} - G_{D_q^{(*)}}(m_p) \right] - 2F_2 C_{8g}^{\text{eff}} \right\}, \\ P_8^p &= \frac{\alpha_e}{9\pi} \frac{1}{N_c} \left\{ (C_1 + N_c C_2) \left[\frac{10}{9} - G_{D_q^{(*)}}(m_p) \right] - 3F_2 C_{7\gamma}^{\text{eff}} \right\}, \\ P_{10}^p &= \frac{\alpha_e}{9\pi} \frac{1}{N_c} \left\{ (C_1 + N_c C_2) \left[\frac{10}{9} - G_{D_q^{(*)}}(m_p) \right] - 3F_1 C_{7\gamma}^{\text{eff}} \right\}, \end{aligned} \quad (13)$$

where the penguin loop-integral function $G_{D_q^{(*)}}(m_p)$ is given by

$$G_{D_q^{(*)}}(m_p) = \int_0^1 du G(m_p, k) \Phi_{D_q^{(*)}}(u), \quad (14)$$

$$G(m_p, k) = -4 \int_0^1 dx x(1-x) \ln \left[\frac{m_p^2 - k^2 x(1-x)}{m_b^2} - i\epsilon \right], \quad (15)$$

with the penguin momentum transfer $k^2 = m_c^2 + \bar{u}(m_b^2 - m_c^2 - m_{M_2}^2) + \bar{u}^2 m_{M_2}^2$, where $\bar{u} \equiv 1 - u$. In the function $G_{D_q^{(*)}}(m_p)$, we have used a $D_q^{(*)}$ meson-emitting distribution amplitude $\Phi_{D_q^{(*)}}(u) = 6u(1-u)[1 + a_{D_q^{(*)}}(1-2u)]$, in stead of keeping k^2 as a free parameter as usual.

The constants F_1 and F_2 in Eq. (13) are defined by

$$F_1 = \begin{cases} \int_0^1 du \Phi_{D_q}(u) \frac{m_b}{m_b - m_c} \frac{m_b^2 - um_{D_q}^2 - 2m_c^2 + m_b m_c}{k^2} & (DD_q), \\ \int_0^1 du \Phi_{D_q^*}(u) \frac{m_b}{k^2} \left(\bar{u} m_b + \frac{2um_{D_q^*}}{m_b - m_c} \epsilon_2^* \cdot p_1 - um_c \right) & (DD_q^*), \\ \int_0^1 du \Phi_{D_q}(u) \frac{m_b}{m_b + m_c} \frac{m_b^2 - um_{D_q}^2 - 2m_c^2 - m_b m_c}{k^2} & (D^*D_q), \\ \int_0^1 du \Phi_{D_q^*}(u) \frac{m_b}{k^2} \left(\bar{u} m_b + \frac{2um_{D_q^*}}{m_b + m_c} \epsilon_2^* \cdot p_1 + um_c \right) & (D^*D_q^*), \end{cases} \quad (16)$$

$$F_2 = \begin{cases} \int_0^1 du \Phi_{D_q}(u) \frac{m_b}{k^2} [\bar{u}(m_b - m_c) + m_c] & (DD_q), \\ 0 & (DD_q^*), \\ \int_0^1 du \Phi_{D_q}(u) \frac{m_b}{k^2} [\bar{u}(m_b + m_c) - m_c] & (D^*D_q), \\ 0 & (D^*D_q^*), \end{cases} \quad (17)$$

where $\epsilon_{2L}^* \cdot p_1 \approx (m_b^2 - m_{M_q^*}^2 - m_c^2)/(2m_{M_q^*})$ and $\epsilon_{2T}^* \cdot p_1 = 0$ for $B \rightarrow D^* D_q^*$ decays.

2.2 Decay amplitudes of the RPV contributions

In the RPV MSSM, in terms of the RPV superpotential [17], we can obtain the relative RPV effective Hamiltonian for $B \rightarrow D^{(*)} D_q^{(*)}$ decays as following

$$\begin{aligned} \mathcal{H}_{\text{eff}}^{\text{RPV}} &= \sum_n \frac{\lambda''_{ikn} \lambda''_{jln}^*}{2m_{\tilde{d}_n}^2} \eta^{-4/\beta_0} \left[-(\bar{d}_k \gamma^\mu P_R u_j)_1 (\bar{u}_i \gamma_\mu P_R d_l)_1 + (\bar{d}_k \gamma^\mu P_R u_j)_8 (\bar{u}_i \gamma_\mu P_R d_l)_8 \right] \\ &+ \sum_i \frac{\lambda'_{ijk} \lambda'_{inl}^*}{m_{\tilde{e}_{iL}}^2} \eta^{-8/\beta_0} (\bar{d}_k P_L u_j)_1 (\bar{u}_n P_R d_l)_1 + h.c., \end{aligned} \quad (18)$$

where $P_L = \frac{1-\gamma_5}{2}$, $P_R = \frac{1+\gamma_5}{2}$, $\eta = \frac{\alpha_s(m_{\tilde{f}})}{\alpha_s(m_b)}$ and $\beta_0 = 11 - \frac{2}{3}n_f$. The subscripts 1 and 8 of the currents represent the currents in the color singlet and octet, respectively. The coefficients η^{-4/β_0} and η^{-8/β_0} are due to the running from sfermion mass scale $m_{\tilde{f}}$ (assumed as 100 GeV) down to m_b scale. Since it is usually assumed in phenomenology for numerical display that only one sfermion contributes at one time, we neglect the mixing between the operators when we use the renormalization group equation (RGE) to run $\mathcal{H}_{\text{eff}}^{\text{RPV}}$ down to the low scale.

The decay amplitudes of RPV contributions to $B \rightarrow D^{(*)} D_q^{(*)}$ are given by

$$\begin{aligned} \mathcal{M}^{\text{RPV}}(B \rightarrow D^{(*)} D_q^{(*)}) &= \Lambda'' \left(-1 + \frac{1}{N_C} \right) \langle D_q^{(*)} | \bar{q} \gamma_\mu (1 + \gamma_5) c | 0 \rangle \langle D^{(*)} | \bar{c} \gamma_\mu (1 + \gamma_5) b | B \rangle \\ &\quad + 2\Lambda' \langle D_q^{(*)} | \bar{q} (1 - \gamma_5) c | 0 \rangle \langle D^{(*)} | \bar{c} (1 + \gamma_5) b | B \rangle, \end{aligned} \quad (19)$$

$$= \begin{cases} \left[-\Lambda'' \left(-1 + \frac{1}{N_C} \right) + \xi \Lambda' \right] A_{[BD, D_q]} & (DD_q), \\ \left[\Lambda'' \left(-1 + \frac{1}{N_C} \right) \right] A_{[BD, D_q^*]} & (DD_q^*), \\ \left[\Lambda'' \left(-1 + \frac{1}{N_C} \right) - \xi \Lambda' \right] A_{[BD^*, D_q]} & (D^* D_q), \\ \left[\Lambda'' \left(-1 + \frac{1}{N_C} \right) \right] A'_{[BD^*, D_q^*]} & (D^* D_q^*), \end{cases} \quad (20)$$

where $\Lambda'' \equiv \eta^{-4/\beta_0} \frac{\lambda_{232}'' \lambda_{212}''}{8m_s^2} \left(\frac{\lambda_{231}'' \lambda_{221}''}{8m_d^2} \right)$ and $\Lambda' \equiv \eta^{-8/\beta_0} \sum_i \frac{\lambda_{i23}^* \lambda'_{i21}}{8m_{\tilde{e}_{iL}}^2} \left(\frac{\lambda_{i23}^* \lambda'_{i22}}{8m_{\tilde{e}_{iL}}^2} \right)$ for $q = d$ ($q = s$). $A'_{[BD^*, D_q^*]}$ is defined by

$$\begin{aligned} A'_{[BD^*, D_q^*]} &\equiv if_{D_q^*} m_{D_q^*} \left[(\varepsilon_{D^*}^* \cdot \varepsilon_{D_q^*}^*) (m_B + m_{D^*}) A_1(m_{D_q^*}^2) \right. \\ &\quad \left. - (\varepsilon_{D^*}^* \cdot p_{D_q^*}) (\varepsilon_{D_q^*}^* \cdot p_{D^*}) \frac{2A_2(m_{D_q^*}^2)}{m_B + m_{D^*}} - i\epsilon_{\mu\nu\alpha\beta} \varepsilon_{D_q^*}^{*\mu} \varepsilon_{D^*}^{*\nu} p_{D_q^*}^\alpha p_{D^*}^\beta \frac{2V(m_{D_q^*}^2)}{m_B + m_{D^*}} \right]. \end{aligned} \quad (21)$$

2.3 Observables to be investigated

We can get the total decay amplitudes in the RPV MSSM as

$$\mathcal{M}(B \rightarrow D^{(*)} D_q^{(*)}) = \mathcal{M}^{\text{SM}}(B \rightarrow D^{(*)} D_q^{(*)}) + \mathcal{M}^{\text{RPV}}(B \rightarrow D^{(*)} D_q^{(*)}). \quad (22)$$

The branching ratio \mathcal{B} reads as

$$\mathcal{B}(B \rightarrow D^{(*)} D_q^{(*)}) = \frac{\tau_B |p_c|}{8\pi m_B^2} \left| \mathcal{M}(B \rightarrow D^{(*)} D_q^{(*)}) \right|^2, \quad (23)$$

where τ_B is the B lifetime, $|p_c|$ is the center of mass momentum in the center of mass frame of B meson. In $B \rightarrow D^* D_q^*$ decays, the two vector mesons have the same helicity, therefore three different polarization states, one longitudinal and two transverse, are possible. We define the corresponding amplitudes as $\mathcal{M}_{0,\pm}$ in the helicity basis and $\mathcal{M}_{L,\parallel,\perp}$ in the transversity basis, which are related by $\mathcal{M}_L = \mathcal{M}_0$ and $\mathcal{M}_{\parallel,\perp} = \frac{\mathcal{M}_{\pm} \pm \mathcal{M}_{\mp}}{\sqrt{2}}$. Then we have

$$\left| \mathcal{M}(B \rightarrow D^* D_q^*) \right|^2 = |\mathcal{M}_0|^2 + |\mathcal{M}_+|^2 + |\mathcal{M}_-|^2 = |\mathcal{M}_L|^2 + |\mathcal{M}_{\parallel}|^2 + |\mathcal{M}_{\perp}|^2. \quad (24)$$

The longitudinal polarization fraction f_L and transverse polarization fraction f_{\perp} are defined by

$$f_{L,\perp}(B \rightarrow D^* D_q^*) = \frac{\Gamma_{L,\perp}}{\Gamma} = \frac{|\mathcal{M}_{L,\perp}|^2}{|\mathcal{M}_L|^2 + |\mathcal{M}_{\parallel}|^2 + |\mathcal{M}_{\perp}|^2}. \quad (25)$$

In charged B meson decays, where mixing effects are absent, the only possible source of CPAs is

$$\mathcal{A}_{\text{CP}}^{k,\text{dir}} = \frac{|\mathcal{M}_k(B^- \rightarrow \bar{f})/\mathcal{M}_k(B^+ \rightarrow f)|^2 - 1}{|\mathcal{M}_k(B^- \rightarrow \bar{f})/\mathcal{M}_k(B^+ \rightarrow f)|^2 + 1}, \quad (26)$$

and $k = L, \parallel, \perp$ for $B^- \rightarrow D^*D_q^*$ decays and $k = L$ for $B_u^- \rightarrow DD_q, DD_q^*, D^*D_q$ decays. Then for $B_u^- \rightarrow D^*D_q^*$ decays, we have

$$\mathcal{A}_{\text{CP}}^{+,\text{dir}}(B \rightarrow D^*D_q^*) = \frac{\mathcal{A}_{\text{CP}}^{\parallel,\text{dir}}|\mathcal{M}_{\parallel}|^2 + \mathcal{A}_{\text{CP}}^{L,\text{dir}}|\mathcal{M}_L|^2}{|\mathcal{M}_{\parallel}|^2 + |\mathcal{M}_L|^2}. \quad (27)$$

For CPAs of neutral B_q meson decays, there is an additional complication due to $B_q^0 - \bar{B}_q^0$ mixing. There are four cases that one encounters for neutral B_q decays, as discussed in Refs. [38, 39, 40, 41].

- (i) $B_q^0 \rightarrow f, \bar{B}_q^0 \rightarrow \bar{f}$, where f or \bar{f} is not a common final state of B_q^0 and \bar{B}_q^0 , for example $B_q^0 \rightarrow D^+D_s^-$.
- (ii) $B_q^0 \rightarrow (f = \bar{f}) \leftarrow \bar{B}_q^0$ with $f^{\text{CP}} = \pm f$, involving final states which are CP eigenstates, *i.e.*, decays such as $B_d^0 \rightarrow D^+D^-, B_s^0 \rightarrow D_s^+D_s^-$.
- (iii) $B_q^0 \rightarrow (f = \bar{f}) \leftarrow \bar{B}_q^0$ with $f^{\text{CP}} \neq \pm f$, involving final states which are not CP eigenstates. They include decays such as $B_q^0 \rightarrow (VV)^0$, as the VV states are not CP eigenstates.
- (iv) $B_q^0 \rightarrow (f \& \bar{f}) \leftarrow \bar{B}_q^0$ with $f^{\text{CP}} \neq f$, *i.e.*, both f and \bar{f} are common final states of B_q^0 and \bar{B}_q^0 , but they are not CP eigenstates. Decays $B_d^0(\bar{B}_d^0) \rightarrow D^{*-}D^+, D^-D^{*+}$ and $B_s^0(\bar{B}_s^0) \rightarrow D_s^{*-}D_s^+, D_s^-D_s^{*+}$ belong to this case.

CPAs of neutral B decays in case (i) are similar to CPAs of the charged B decays, and there are only direct CPAs $\mathcal{A}_{\text{CP}}^{\text{dir}}$ since no mixing is involved for these decays. For cases (ii) and (iii), their CPAs would involve $B_q^0 - \bar{B}_q^0$ mixing. The time-dependent asymmetries can be conveniently expressed as

$$\mathcal{A}_f^k(t) = \mathcal{S}_f^k \sin(\Delta mt) - \mathcal{C}_f^k \cos(\Delta mt), \quad (28)$$

$$\mathcal{S}_f^k \equiv \frac{2\text{Im}(\lambda_k)}{1 + |\lambda_k|^2}, \quad \mathcal{C}_f^k \equiv \frac{1 - |\lambda_k|^2}{1 + |\lambda_k|^2}, \quad (29)$$

where $\lambda_k = \frac{q}{p} \frac{\mathcal{M}_k(\bar{B}^0 \rightarrow f)}{\mathcal{M}_k(B^0 \rightarrow f)}$. In addition, \mathcal{S}_f^+ and \mathcal{C}_f^+ can be obtained from the similar relation given in Eq. (27).

Case (iv) also involves mixing but requires additional formulae. Here one studies the four time-dependent decay widths for $B_q^0(t) \rightarrow f$, $\bar{B}_q^0(t) \rightarrow \bar{f}$, $B_q^0(t) \rightarrow \bar{f}$ and $\bar{B}_q^0(t) \rightarrow f$ [38, 39, 40, 41]. These time-dependent widths can be expressed by four basic matrix elements [40]

$$\begin{aligned} g &= \langle f | \mathcal{H}_{eff} | B_q^0 \rangle, & h &= \langle f | \mathcal{H}_{eff} | \bar{B}_q^0 \rangle, \\ \bar{g} &= \langle \bar{f} | \mathcal{H}_{eff} | \bar{B}_q^0 \rangle, & \bar{h} &= \langle \bar{f} | \mathcal{H}_{eff} | B_q^0 \rangle, \end{aligned} \quad (30)$$

which determine the decay matrix elements of $B_q^0 \rightarrow f, \bar{f}$ and of $\bar{B}_q^0 \rightarrow f, \bar{f}$ at $t = 0$. We will study the following quantities

$$\mathcal{S}_f^k = \frac{2\text{Im}(\lambda'_k)}{1 + |\lambda'_k|^2}, \quad \mathcal{C}_f^k = \frac{1 - |\lambda'_k|^2}{1 + |\lambda'_k|^2}, \quad (31)$$

$$\mathcal{S}_{\bar{f}}^k = \frac{2\text{Im}(\lambda''_k)}{1 + |\lambda''_k|^2}, \quad \mathcal{C}_{\bar{f}}^k = \frac{1 - |\lambda''_k|^2}{1 + |\lambda''_k|^2}, \quad (32)$$

with $\lambda'_k = (q/p)(h/g)$ and $\lambda''_k = (q/p)(\bar{g}/\bar{h})$. The signatures of CP violation are $\Gamma(\bar{B}_q^0(t) \rightarrow \bar{f}) \neq \Gamma(B_q^0(t) \rightarrow f)$ and $\Gamma(\bar{B}_q^0(t) \rightarrow f) \neq \Gamma(B_q^0(t) \rightarrow \bar{f})$, which means that $\mathcal{C}_f \neq -\mathcal{C}_{\bar{f}}$ and/or $\mathcal{S}_f \neq -\mathcal{S}_{\bar{f}}$.

2.4 Input parameters

Theoretical input parameters are collected in Table 1. In our numerical results, we will use the input parameters which are varied randomly within 1σ range.

We have several remarks on the input parameters:

- CKM matrix elements: The weak phase γ is well constrained in the SM, however, with the presence of R-parity violation, this constraint may be relaxed. We will not take γ within the SM range, but vary it randomly in the range of 0 to π to obtain conservative limits on RPV couplings.
- Decay constants: The decay constants of D_q^* mesons have not been directly measured in experiments so far. In the heavy-quark limit ($m_c \rightarrow \infty$), spin symmetry predicts that $f_{D_q^*} = f_{D_q}$, and most theoretical predictions indicate that symmetry-breaking corrections enhance the ratio $f_{D_q^*}/f_{D_q}$ by 10% – 20% [45, 46]. Hence, we take $f_{D_q^*} = (1.1 - 1.2)f_{D_q}$ as our input values.
- Distribution amplitudes: The distribution amplitudes of $D_q^{(*)}$ mesons are less constrained, and we use the shape parameter $a_{D^{(*)}} = 0.7 \pm 0.2$ and $a_{D_s^{(*)}} = 0.3 \pm 0.2$.

Table 1: Summary of theoretical input parameters and $\pm 1\sigma$ error ranges for sensitive parameters used in our numerical calculations.

$m_{B_u} = 5.279 \text{ GeV}, m_{B_d} = 5.280 \text{ GeV}, m_{B_s} = 5.366 \text{ GeV}, M_{D^0} = 1.865 \text{ GeV},$ $M_{D^+} = 1.870 \text{ GeV}, M_{D_s^+} = 1.969 \text{ GeV}, M_{D^{*0}} = 2.007 \text{ GeV}, M_{D^{*+}} = 2.010 \text{ GeV},$ $M_{D_s^{*+}} = 2.107 \text{ GeV}, \bar{m}_b(\bar{m}_b) = (4.20 \pm 0.07) \text{ GeV}, \bar{m}_c(\bar{m}_c) = (1.25 \pm 0.09) \text{ GeV},$ $\bar{m}_s(2 \text{ GeV}) = (0.095 \pm 0.025) \text{ GeV}, \bar{m}_u(2 \text{ GeV}) = (0.0015 \sim 0.0030) \text{ GeV},$ $\bar{m}_d(2 \text{ GeV}) = (0.003 \sim 0.007) \text{ GeV},$ $\tau_{B_u} = (1.638 \pm 0.011) \text{ ps}, \tau_{B_d} = (1.530 \pm 0.009) \text{ ps}, \tau_{B_s} = (1.425_{-0.041}^{+0.041}) \text{ ps}.$	[42]
$ V_{ud} = 0.97430 \pm 0.00019, V_{us} = 0.22521_{-0.00082}^{+0.00083}, V_{ub} = 0.00344_{-0.00017}^{+0.00022},$ $ V_{cd} = 0.22508_{-0.00082}^{+0.00084}, V_{cs} = 0.97350_{-0.00022}^{+0.00021}, V_{cb} = 0.04045_{-0.00078}^{+0.00106},$ $ V_{td} = 0.00841_{-0.00092}^{+0.00035}, V_{ts} = 0.03972_{-0.00077}^{+0.00115}, V_{tb} = 0.999176_{-0.000044}^{+0.000031},$ $\alpha = (90.7_{-2.9}^{+4.5})^\circ, \beta = (21.7_{-0.9}^{+1.0})^\circ, \gamma = (67.6_{-4.5}^{+2.8})^\circ.$	[43]
$f_D = (0.201 \pm 0.003 \pm 0.017) \text{ GeV}, f_{D_s} = (0.249 \pm 0.003 \pm 0.016) \text{ GeV}.$	[44]

- Form factors: For the form factors involving $B \rightarrow D^{(*)}$ transitions, we take expressions which include perturbative QCD corrections induced by hard gluon vertex corrections of $b \rightarrow c$ transitions and power corrections in orders of $1/m_{b,c}$ [37, 47]. As for Isgur-Wise function $\xi(\omega)$, we use the fit result $\xi(\omega) = 1 - 1.22(\omega - 1) + 0.85(\omega - 1)^2$ from Ref. [48].
- Wilson coefficients: We obtain Wilson coefficients in terms of the expressions in [35].
- RPV couplings: When we study the RPV effects, we consider only one RPV coupling product contributes at one time, neglecting the interferences between different RPV coupling products, but keeping their interferences with the SM amplitude. We assume the masses of sfermion are 100 GeV. For other values of the sfermion masses, the bounds on the couplings in this paper can be easily obtained by scaling them by factor $\tilde{f}^2 \equiv (\frac{m_{\tilde{f}}}{100 \text{ GeV}})^2$.

3 Numerical results and discussions

In this section we summarize our numerical results and analysis in the exclusive color-allowed $b \rightarrow c\bar{c}q$ decays. First, we will show our estimates in the SM with full theoretical uncertainties of sensitive parameters. Then, we will investigate the RPV effects in the decays. We will constrain

relevant RPV couplings only from quite highly consistent experimental data and show the RPV MSSM predictions for the other observables, which have not been measured yet or have less consistency among different collaborations.

3.1 Exclusive color-allowed $b \rightarrow c\bar{c}d$ decays

Decays $\bar{B}_d^0 \rightarrow D^{(*)+} D^{(*)-}$, $B_u^- \rightarrow D^{(*)0} D^{(*)-}$ and $\bar{B}_s^0 \rightarrow D_s^{(*)+} D^{(*)-}$ are dominated by the color-allowed $b \rightarrow c\bar{c}d$ tree diagram, but involve small penguin pollution from the $b \rightarrow u\bar{u}d$ transition carrying a different weak phase. These decays involve the same set of RPV coupling constants $\lambda_{232}^{l*} \lambda_{212}^{l''}$ and $\lambda_{i23}^{l*} \lambda_{i21}^{l'}$ at tree level due to squark and slepton exchanges, respectively. For $\bar{B}_d^0 \rightarrow D^{(*)+} D^{(*)-}$ and $B_u^- \rightarrow D^{(*)0} D^{(*)-}$ processes, a few observables have been measured by BABAR and Belle collaborations. The latest experimental data and their weight averages are summarized in Table 2. We can see almost all physical quantities have been consistently measured between BABAR and Belle, and only $\mathcal{B}(\bar{B}_d^0 \rightarrow D^+ D^-, D^{*\pm} D^\mp)$, $\mathcal{C}(\bar{B}_d^0 \rightarrow D^+ D^-)$ and $\mathcal{C}(B_d^0, \bar{B}_d^0 \rightarrow D^+ D^{*-})$ have low consistency between BABAR and Belle.

Our SM estimates predicted within the theoretical uncertainties of input parameters are given in the second columns of Table 3 and Table 4. Theoretical predictions for the branching ratios and the polarization fractions are given in Table 3. CPA predictions are given in Table 4. All the branching ratios are above 10^{-4} order. The direct CPAs are expected to be quite small. All mixing-induced CPAs of \bar{B}_d^0 decays are very large (about -0.7). There is an obvious signature of the mixing-induced CP violations in $\bar{B}_s^0 \rightarrow D_s^{*+} D_s^-, D_s^+ D_s^{*-}$ decays since $\mathcal{S}(B_s^0, \bar{B}_s^0 \rightarrow D_s^{*+} D_s^-) \neq -\mathcal{S}(B_s^0, \bar{B}_s^0 \rightarrow D_s^+ D_s^{*-})$, which are consistent with the experimental measurements. In addition, for $\bar{B}_d^0 \rightarrow D^{*+} D^{*-}$, $B_u^- \rightarrow D^{*0} D^{*-}$ and $\bar{B}_s^0 \rightarrow D_s^{*+} D^{*-}$ decays, the longitudinal and transverse polarization fractions can be precisely predicted, and are about ~ 0.5 and ~ 0.1 , respectively. Comparing present experimental data in Table 2 with the SM predictions in Table 3 and Table 4, we can find that all measured quantities agree with the SM expectations within the error ranges except $\mathcal{C}(B_d^0, \bar{B}_d^0 \rightarrow D^+ D^-)$ from Belle.

We now turn to explore the RPV effects in $\bar{B}_d^0 \rightarrow D^{(*)+} D^{(*)-}$, $B_u^- \rightarrow D^{(*)0} D^{(*)-}$ and $\bar{B}_s^0 \rightarrow D_s^{(*)+} D^{(*)-}$ decays. The most conservative existing experimental bounds are used in our analysis. We choose the averaged data, which have highly consistent measurements between BABAR and Belle (defined as a scale factor $S \leq 1$), and varied randomly within 2σ ranges to constrain the RPV effects. The current experimental data and theoretical input parameters are not yet precise enough to set absolute bounds on the relative RPV couplings. We obtain the

Table 2: Experimental data for $\bar{B}_d^0 \rightarrow D^{(*)+} D^{(*)-}$ and $B_u^- \rightarrow D^{(*)0} D^{(*)-}$ decays from BABAR and Belle. The branching ratios (\mathcal{B}) are in units of 10^{-4} . The scale factor S is defined in introduction part of Ref. [42], and $S > 1$ often indicates that the measurements are inconsistent.

Observable	BABAR	Belle	Average	S
$\mathcal{B}(\bar{B}_d^0 \rightarrow D^+ D^-)$	$2.8 \pm 0.4 \pm 0.5$ [9]	$1.97 \pm 0.20 \pm 0.20$ [3]	2.1 ± 0.3	1.2
$\mathcal{B}(\bar{B}_d^0 \rightarrow D^{*+} D^{\mp})$	$5.7 \pm 0.7 \pm 0.7$ [9]	$11.7 \pm 2.6_{-2.5}^{+2.2}$ [26]	6.1 ± 1.5	1.6
$\mathcal{B}(\bar{B}_d^0 \rightarrow D^{*+} D^{*-})$	$8.1 \pm 0.6 \pm 1.0$ [9]	$8.1 \pm 0.8 \pm 1.1$ [7]	8.1 ± 0.9	≤ 1.0
$\mathcal{B}(B_u^- \rightarrow D^0 D^-)$	$3.8 \pm 0.6 \pm 0.5$ [9]	$3.85 \pm 0.31 \pm 0.38$ [10]	3.8 ± 0.4	≤ 1.0
$\mathcal{B}(B_u^- \rightarrow D^{*0} D^-)$	$6.3 \pm 1.4 \pm 1.0$ [9]			
$\mathcal{B}(B_u^- \rightarrow D^0 D^{*-})$	$3.6 \pm 0.5 \pm 0.4$ [9]	$4.57 \pm 0.71 \pm 0.56$ [11]	3.9 ± 0.5	≤ 1.0
$\mathcal{B}(B_u^- \rightarrow D^{*0} D^{*-})$	$8.1 \pm 1.2 \pm 1.2$ [9]			
$\mathcal{C}(\bar{B}_d^0 \rightarrow D^+ D^-)$	$-0.07 \pm 0.23 \pm 0.03$ [4]	$-0.91 \pm 0.23 \pm 0.06$ [3]	-0.48 ± 0.42	2.5
$\mathcal{C}(B_d^0, \bar{B}_d^0 \rightarrow D^{*+} D^-)$	$0.08 \pm 0.17 \pm 0.04$ [4]	$-0.37 \pm 0.22 \pm 0.06$ [5]	-0.09 ± 0.22	1.6
$\mathcal{C}(B_d^0, \bar{B}_d^0 \rightarrow D^+ D^{*-})$	$0.00 \pm 0.17 \pm 0.03$ [4]	$0.23 \pm 0.25 \pm 0.06$ [5]	0.07 ± 0.14	≤ 1.0
$\mathcal{C}^+(\bar{B}_d^0 \rightarrow D^{*+} D^{*-})$	$0.00 \pm 0.12 \pm 0.02$ [4]	$-0.15 \pm 0.13 \pm 0.04$ [8]	-0.07 ± 0.09	≤ 1.0
$\mathcal{A}_{\text{CP}}^{\text{dir}}(B_u^- \rightarrow D^0 D^-)$	$-0.13 \pm 0.14 \pm 0.02$ [9]	$0.00 \pm 0.08 \pm 0.02$ [10]	-0.03 ± 0.07	≤ 1.0
$\mathcal{A}_{\text{CP}}^{\text{dir}}(B_u^- \rightarrow D^{*0} D^-)$	$0.13 \pm 0.18 \pm 0.04$ [9]			
$\mathcal{A}_{\text{CP}}^{\text{dir}}(B_u^- \rightarrow D^0 D^{*-})$	$-0.06 \pm 0.13 \pm 0.02$ [9]	$0.15 \pm 0.15 \pm 0.05$ [11]	0.03 ± 0.10	≤ 1.0
$\mathcal{A}_{\text{CP}}^{+, \text{dir}}(B_u^- \rightarrow D^{*0} D^{*-})$	$-0.15 \pm 0.11 \pm 0.02$ [9]			
$\mathcal{S}(\bar{B}_d^0 \rightarrow D^+ D^-)$	$-0.63 \pm 0.36 \pm 0.05$ [4]	$-1.13 \pm 0.37 \pm 0.09$ [3]	-0.87 ± 0.26	≤ 1.0
$\mathcal{S}(B_d^0, \bar{B}_d^0 \rightarrow D^{*+} D^-)$	$-0.62 \pm 0.21 \pm 0.03$ [4]	$-0.55 \pm 0.39 \pm 0.12$ [5]	-0.61 ± 0.19	≤ 1.0
$\mathcal{S}(B_d^0, \bar{B}_d^0 \rightarrow D^+ D^{*-})$	$-0.73 \pm 0.23 \pm 0.05$ [4]	$-0.96 \pm 0.43 \pm 0.12$ [5]	-0.78 ± 0.21	≤ 1.0
$\mathcal{S}^+(\bar{B}_d^0 \rightarrow D^{*+} D^{*-})$	$-0.76 \pm 0.16 \pm 0.04$ [4]	$-0.96 \pm 0.25_{-0.16}^{+0.12}$ [8]	-0.81 ± 0.14	≤ 1.0
$f_{\perp}(\bar{B}_d^0 \rightarrow D^{*+} D^{*-})$	$0.158 \pm 0.028 \pm 0.006$ [4]	$0.125 \pm 0.043 \pm 0.023$ [8]	0.150 ± 0.025	≤ 1.0
$f_L(\bar{B}_d^0 \rightarrow D^{*+} D^{*-})$		$0.57 \pm 0.08 \pm 0.02$ [7]		

allowed scattering spaces of the RPV couplings $\lambda_{232}^{\prime*} \lambda_{212}^{\prime\prime}$ and $\lambda_{i23}^{\prime*} \lambda_{i21}^{\prime}$ as displayed in Fig. 1. These survived parameter spaces are not in conflict with the above mentioned highly consistent experimental data in $\bar{B}_d^0 \rightarrow D^{(*)+} D^{(*)-}$ and $B_u^- \rightarrow D^{(*)0} D^{(*)-}$ decays.

The squark exchange coupling $\lambda_{232}^{\prime*} \lambda_{212}^{\prime\prime}$ contributes to all twelve $\bar{B}_d^0 \rightarrow D^{(*)+} D^{(*)-}$, $B_u^- \rightarrow D^{(*)0} D^{(*)-}$ and $\bar{B}_s^0 \rightarrow D_s^{(*)+} D^{(*)-}$ decay modes. The allowed space of $\lambda_{232}^{\prime*} \lambda_{212}^{\prime\prime}$ is shown in the left plot of Fig. 1. Its magnitude $|\lambda_{232}^{\prime*} \lambda_{212}^{\prime\prime}|$ and its RPV weak phase ϕ_{RPV} have been constrained significantly. We obtain $|\lambda_{232}^{\prime*} \lambda_{212}^{\prime\prime}| \in [0.14, 1.62] \times 10^{-3}$ and $\phi_{\text{RPV}} \in [-75^\circ, 84^\circ]$. The right plot of Fig. 1 displays the allowed space of the RPV couplings $\lambda_{i23}^{\prime*} \lambda_{i21}^{\prime}$ due to slepton exchanges, which

Table 3: Theoretical predictions for CP-averaged branching ratios (in units of 10^{-4}) and ratios of polarization (in units of 10^{-2}) in exclusive color-allowed $b \rightarrow c\bar{c}d$ decays. The second column gives the SM predictions with the theoretical uncertainties of input parameters. The last two columns are the RPV MSSM predictions with different RPV couplings considering the input parameter uncertainties and experimental errors.

Observable	SM	MSSM w/ $\lambda''_{232}\lambda''_{212}$	MSSM w/ $\lambda'_{i23}\lambda'_{i21}$
$\mathcal{B}(\bar{B}_d^0 \rightarrow D^+D^-)$	[2.35, 4.15]	[2.77, 3.80]	[2.77, 4.39]
$\mathcal{B}(\bar{B}_d^0 \rightarrow D^{*+}D^-)$	[2.27, 3.96]	[2.87, 4.22]	[2.30, 4.59]
$\mathcal{B}(\bar{B}_d^0 \rightarrow D^+D^{*-})$	[2.56, 5.04]	[3.31, 4.65]	
$\mathcal{B}(\bar{B}_d^0 \rightarrow D^{*\pm}D^\mp)$	[4.84, 8.95]	[6.18, 8.70]	[5.21, 8.84]
$\mathcal{B}(\bar{B}_d^0 \rightarrow D^{*+}D^{*-})$	[6.21, 12.22]	[7.05, 8.90]	
$\mathcal{B}(B_u^- \rightarrow D^0D^-)$	[2.53, 4.43]	[3.00, 4.04]	[3.00, 4.68]
$\mathcal{B}(B_u^- \rightarrow D^{*0}D^-)$	[2.42, 4.27]	[3.07, 4.53]	[2.25, 4.75]
$\mathcal{B}(B_u^- \rightarrow D^0D^{*-})$	[2.73, 5.42]	[3.55, 4.96]	
$\mathcal{B}(B_u^- \rightarrow D^{*0}D^{*-})$	[6.61, 13.10]	[7.54, 10.67]	
$\mathcal{B}(\bar{B}_s^0 \rightarrow D_s^+D^-)$	[2.33, 4.20]	[2.76, 3.81]	[2.77, 4.48]
$\mathcal{B}(\bar{B}_s^0 \rightarrow D_s^{*+}D^-)$	[2.24, 4.00]	[2.81, 4.25]	[2.08, 4.42]
$\mathcal{B}(\bar{B}_s^0 \rightarrow D_s^+D^{*-})$	[2.54, 5.03]	[3.27, 4.69]	
$\mathcal{B}(\bar{B}_s^0 \rightarrow D_s^{*+}D^{*-})$	[6.15, 12.10]	[6.92, 10.04]	
$f_L(\bar{B}_d^0 \rightarrow D^{*+}D^{*-})$	[52.40, 52.97]	[50.35, 52.53]	
$f_L(B_u^- \rightarrow D^{*0}D^{*-})$	[52.43, 53.02]	[50.37, 52.56]	
$f_L(\bar{B}_s^0 \rightarrow D_s^{*+}D^{*-})$	[52.56, 53.16]	[50.60, 52.70]	
$f_\perp(\bar{B}_d^0 \rightarrow D^{*+}D^{*-})$	[8.82, 9.51]	[10.00, 12.94]	
$f_\perp(B_u^- \rightarrow D^{*0}D^{*-})$	[8.84, 9.53]	[10.03, 12.97]	
$f_\perp(\bar{B}_s^0 \rightarrow D_s^{*+}D^{*-})$	[8.35, 9.05]	[9.50, 12.34]	

contributes only to six decay modes $\bar{B}_d^0 \rightarrow D^{(*)+}D^-$, $B_u^- \rightarrow D^{(*)0}D^-$ and $\bar{B}_s^0 \rightarrow D_s^{(*)+}D^-$. The magnitudes $|\lambda'_{i23}\lambda'_{i21}|$ have been limited within $|\lambda'_{i23}\lambda'_{i21}| \leq 1.28 \times 10^{-3}$, and the corresponding RPV weak phase ϕ_{RPV} for the range $|\lambda'_{i23}\lambda'_{i21}| \leq 0.4 \times 10^{-3}$ is not constrained so much, however, the RPV weak phase for $|\lambda'_{i23}\lambda'_{i21}| \in [0.4, 1.3] \times 10^{-3}$ is very narrow.

Using the constrained parameter spaces shown in Fig. 1, one may predict the RPV effects

Table 4: Theoretical predictions for CPAs (in units of 10^{-2}) in exclusive color-allowed $b \rightarrow c\bar{c}d$ decays.

Observable	SM	MSSM w/ $\lambda''_{232} \lambda''_{212}$	MSSM w/ $\lambda'_{i23} \lambda'_{i21}$
$\mathcal{S}(B_d^0, \bar{B}_d^0 \rightarrow D^+ D^-)$	$[-78.00, -71.67]$	$[-97.52, -52.66]$	$[-99.83, -35.16]$
$\mathcal{S}(B_d^0, \bar{B}_d^0 \rightarrow D^{*+} D^-)$	$[-70.40, -64.55]$	$[-81.77, -32.17]$	$[-98.01, -55.02]$
$\mathcal{S}(B_d^0, \bar{B}_d^0 \rightarrow D^+ D^{*-})$	$[-72.17, -66.83]$	$[-83.29, -36.15]$	$[-98.30, -57.69]$
$\mathcal{S}^+(B_d^0, \bar{B}_d^0 \rightarrow D^{*+} D^{*-})$	$[-72.73, -67.77]$	$[-95.18, -53.01]$	
$\mathcal{C}(B_d^0, \bar{B}_d^0 \rightarrow D^+ D^-)$	$[-6.03, -3.87]$	$[-7.61, 0.92]$	$[-11.05, 2.59]$
$\mathcal{C}(B_d^0, \bar{B}_d^0 \rightarrow D^{*+} D^-)$	$[3.36, 13.83]$	$[1.38, 14.75]$	$[-13.35, 21.30]$
$\mathcal{C}(B_d^0, \bar{B}_d^0 \rightarrow D^+ D^{*-})$	$[-14.44, -3.53]$	$[-14.83, -1.45]$	$[-21.00, 13.28]$
$\mathcal{C}^+(B_d^0, \bar{B}_d^0 \rightarrow D^{*+} D^{*-})$	$[-1.35, -1.03]$	$[-1.83, 0.20]$	
$\mathcal{A}_{\text{CP}}^{\text{dir}}(B_u^- \rightarrow D^0 D^-)$	$[3.87, 6.03]$	$[-0.92, 7.61]$	$[-2.59, 11.05]$
$\mathcal{A}_{\text{CP}}^{\text{dir}}(B_u^- \rightarrow D^{*0} D^-)$	$[-1.15, -0.45]$	$[-1.10, 0.29]$	$[-1.99, 0.23]$
$\mathcal{A}_{\text{CP}}^{\text{dir}}(B_u^- \rightarrow D^0 D^{*-})$	$[1.03, 1.35]$	$[-0.40, 1.42]$	
$\mathcal{A}_{\text{CP}}^{+, \text{dir}}(B_u^- \rightarrow D^{*0} D^{*-})$	$[1.03, 1.35]$	$[-0.20, 1.83]$	
$\mathcal{A}_{\text{CP}}^{\text{dir}}(\bar{B}_s^0 \rightarrow D_s^+ D^-)$	$[3.87, 6.03]$	$[-0.92, 7.61]$	$[-2.59, 11.05]$
$\mathcal{A}_{\text{CP}}^{\text{dir}}(\bar{B}_s^0 \rightarrow D_s^{*+} D^-)$	$[-1.15, -0.45]$	$[-1.10, 0.29]$	$[-1.99, 0.23]$
$\mathcal{A}_{\text{CP}}^{\text{dir}}(\bar{B}_s^0 \rightarrow D_s^+ D^{*-})$	$[1.03, 1.35]$	$[-0.40, 1.42]$	
$\mathcal{A}_{\text{CP}}^{+, \text{dir}}(\bar{B}_s^0 \rightarrow D_s^{*+} D^{*-})$	$[1.03, 1.35]$	$[-0.20, 1.83]$	

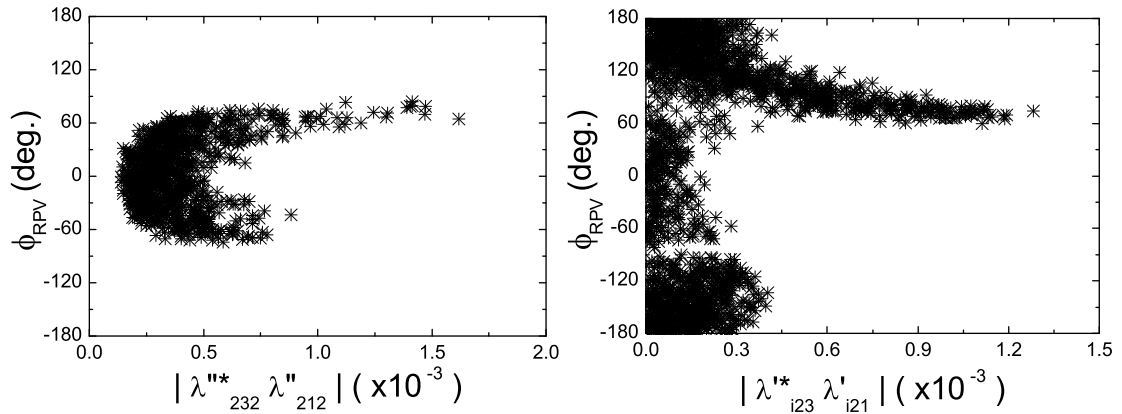


Figure 1: Allowed parameter spaces for relevant RPV couplings constrained by $\bar{B}_d^0 \rightarrow D^{(*)+} D^{(*)-}$ and $B_u^- \rightarrow D^{(*)0} D^{(*)-}$, where ϕ_{RPV} denotes the RPV weak phase.

on the other quantities which have not been measured yet or have less consistent measurements between BABAR and Belle. With the expressions for \mathcal{B} , \mathcal{C} , \mathcal{S} , $\mathcal{A}_{\text{CP}}^{\text{dir}}$, f_L and f_{\perp} at hand, we perform a scan on the input parameters and the constrained RPV couplings. Then we obtain the RPV MSSM predictions with different RPV coupling, whose numerical results are summarized in the last two columns of Table 3 and Table 4.

The contributions of $\lambda_{232}^{\prime\prime*}\lambda_{212}^{\prime\prime}$ due to squark exchange are summarized in the third columns of Table 3 and Table 4. In Table 3, comparing with the SM predictions, we find $\lambda_{232}^{\prime\prime*}\lambda_{212}^{\prime\prime}$ coupling could not affect all branching ratios much. Three $f_L(B \rightarrow D^*D^*)$ and three $f_{\perp}(B \rightarrow D^*D^*)$ are slightly decreased and increased by $\lambda_{232}^{\prime\prime*}\lambda_{212}^{\prime\prime}$ coupling, respectively, and their allowed ranges are scarcely magnified by this coupling. As given in Table 4, the $\lambda_{232}^{\prime\prime*}\lambda_{212}^{\prime\prime}$ contributions could greatly enlarge the ranges of four $\mathcal{S}(B_d^0, \bar{B}_d^0 \rightarrow D^{(*)+}D^{(*)-})$. The effects of $\lambda_{232}^{\prime\prime*}\lambda_{212}^{\prime\prime}$ coupling could extend a little bit the allowed regions of four $\mathcal{C}(B_d^0, \bar{B}_d^0 \rightarrow D^{(*)+}D^{(*)-})$ and eight $\mathcal{A}_{\text{CP}}^{\text{dir}}(B_u^- \rightarrow D^{(*)0}D^{(*)-}, \bar{B}_s^0 \rightarrow D_s^{(*)+}D^{(*)-})$, too. But this squark exchange coupling cannot explain the large $\mathcal{C}(B_d^0, \bar{B}_d^0 \rightarrow D^+D^-)$ from Belle. The predictions including slepton exchange couplings $\lambda_{i23}^*\lambda_{i21}^{\prime}$ are listed in the last columns of Table 3 and Table 4. The $\lambda_{i23}^*\lambda_{i21}^{\prime}$ couplings do not give very big effects on the relevant branching ratios, but could significantly magnify the ranges of $\mathcal{S}(B_d^0, \bar{B}_d^0 \rightarrow D^{(*)+}D^-)$ from their SM predictions as well as extend the ranges of $\mathcal{C}(B_d^0, \bar{B}_d^0 \rightarrow D^{(*)+}D^-)$ and $\mathcal{A}_{\text{CP}}^{\text{dir}}(B_u^- \rightarrow D^{(*)0}D^-, \bar{B}_s^0 \rightarrow D_s^{(*)+}D^-)$. The lower limits of $\mathcal{C}(B_d^0, \bar{B}_d^0 \rightarrow D^{(*)+}D^-)$ could be reduced by these slepton exchange couplings, too, but slepton exchange coupling effects are still not large enough to explain the large $\mathcal{C}(B_d^0, \bar{B}_d^0 \rightarrow D^+D^-)$ from Belle.

It is worth noting that our investigation of the color-allowed $b \rightarrow c\bar{c}d$ decays was motivated by the large direct CPA of $\bar{B}_d^0 \rightarrow D^+D^-$ reported by Belle [3], which has not been confirmed by BABAR and contradicted the SM prediction. Relative RPV couplings, constrained by all consistent measurements in $\bar{B}_d^0 \rightarrow D^{(*)+}D^{(*)-}$ and $B_u^- \rightarrow D^{(*)0}D^{(*)-}$ systems, could slightly enlarge the range of $\mathcal{C}(B_d^0, \bar{B}_d^0 \rightarrow D^+D^-)$. Our RPV MSSM prediction for this observable is coincident with the BABAR measurement, but still cannot explain the Belle measurement. The unparticle interaction has positive effects on $\mathcal{C}(B_d^0, \bar{B}_d^0 \rightarrow D^+D^-)$ as obtained in Ref. [12], in which the author used only experimental constraints of $\mathcal{B}(\bar{B}_d^0 \rightarrow D^+D^-)$. Note also that very large value of $\mathcal{C}(B_d^0, \bar{B}_d^0 \rightarrow D^+D^-)$ could be obtained by unparticle interaction, however, with the sign opposite to the Belle measurement.

For each RPV coupling product, we can present correlations of physical quantities within the

constrained parameter spaces displayed in Fig. 1 by the three-dimensional scatter plots. RPV coupling contributions to $\bar{B}_d^0 \rightarrow D^{(*)+} D^{(*)-}$, $B_u^- \rightarrow D^{(*)0} D^{(*)-}$ and $\bar{B}_s^0 \rightarrow D_s^{(*)+} D^{(*)-}$ decays are very similar to each other. So we will take an example for a few observables of $\bar{B}_d^0 \rightarrow D^{(*)+} D^{(*)-}$ decays to illustrate RPV coupling effects. Effects of RPV couplings $\lambda_{232}'' \lambda_{212}''$ and $\lambda_{i23}^* \lambda_{i21}'$ on observables of $\bar{B}_d^0 \rightarrow D^{(*)+} D^{(*)-}$ decays are shown in Fig. 2 and Fig. 3, respectively.

In Fig. 2, we plot \mathcal{B} , f_L , \mathcal{C} and \mathcal{S} as functions of $\lambda_{232}'' \lambda_{212}''$. Three-dimensional scatter plot Fig. 2 (a) shows $\mathcal{B}(\bar{B}_d^0 \rightarrow D^+ D^-)$ correlated with $|\lambda_{232}'' \lambda_{212}''|$ and its phase ϕ_{RPV} . We also give projections to three perpendicular planes, where the $|\lambda_{232}'' \lambda_{212}''| - \phi_{\text{RPV}}$ plane displays the constrained regions of $\lambda_{232}'' \lambda_{212}''$, as the left plot of Fig. 1. It is shown that $\mathcal{B}(\bar{B}_d^0 \rightarrow D^+ D^-)$ is little decreasing with $|\lambda_{232}'' \lambda_{212}''|$ on the $\mathcal{B} - |\lambda_{232}'' \lambda_{212}''|$ plane. From the $\mathcal{B} - \phi_{\text{RPV}}$ plane, we see that $\mathcal{B}(\bar{B}_d^0 \rightarrow D^+ D^-)$ is not sensitive to ϕ_{RPV} . All other branching ratios have similar trends with $\lambda_{232}'' \lambda_{212}''$ coupling. From Fig. 2 (b-d), we can see $f_L(\bar{B}_d^0 \rightarrow D^{*+} D^{*-})$ and $\mathcal{C}(B_d^0, \bar{B}_d^0 \rightarrow D^+ D^-, D^{*+} D^{*-})$ are not very sensitive with $|\lambda_{232}'' \lambda_{212}''|$ and ϕ_{RPV} . RPV coupling $\lambda_{232}'' \lambda_{212}''$ contributions to $\mathcal{S}(B_d^0, \bar{B}_d^0 \rightarrow D^+ D^-, D^{*+} D^{*-})$ are also very similar to each other. So we take an example for $\mathcal{S}(B_d^0, \bar{B}_d^0 \rightarrow D^+ D^-)$ shown in Fig. 2 (e) to illustrate the RPV coupling effects. $\mathcal{S}(B_d^0, \bar{B}_d^0 \rightarrow D^+ D^-)$ is decreasing (increasing) with $|\lambda_{232}'' \lambda_{212}''|$ when $\phi_{\text{RPV}} > 0$ ($\phi_{\text{RPV}} < 0$), and it is decreasing with ϕ_{RPV} . $\mathcal{S}(B_d^0, \bar{B}_d^0 \rightarrow D^{*+} D^{*-}, D^+ D^{*-})$ have totally different trends to $\mathcal{S}(B_d^0, \bar{B}_d^0 \rightarrow D^+ D^-)$ with $|\lambda_{232}'' \lambda_{212}''|$ and ϕ_{RPV} , and we show only the squark exchange effects on $\mathcal{S}(B_d^0, \bar{B}_d^0 \rightarrow D^{*+} D^-)$ in Fig. 2 (f).

Fig. 3 gives the effects of the slepton exchange couplings $\lambda_{i23}^* \lambda_{i21}'$ in $\bar{B}_d^0 \rightarrow D^{(*)+} D^-$ decays. As displayed in Fig. 3 (a), $\mathcal{B}(\bar{B}_d^0 \rightarrow D^+ D^-)$ is not very sensitive with $|\lambda_{i23}^* \lambda_{i21}'|$ and has only small allowed values when $|\phi_{\text{RPV}}|$ is small. Fig. 3 (b) shows that $\mathcal{B}(\bar{B}_d^0 \rightarrow D^{*+} D^-)$ is decreasing with $|\lambda_{i23}^* \lambda_{i21}'|$ and is weakly sensitive to $|\phi_{\text{RPV}}|$. Fig. 3 (c) exhibits the slepton exchange coupling effects on $\mathcal{C}(B_d^0, \bar{B}_d^0 \rightarrow D^+ D^-)$, which is decreasing with $|\lambda_{i23}^* \lambda_{i21}'|$ and has little sensitivity to ϕ_{RPV} . Slepton exchange couplings have great effects on $\mathcal{C}(B_d^0, \bar{B}_d^0 \rightarrow D^{*+} D^-, D^+ D^{*-})$ and $\mathcal{S}(B_d^0, \bar{B}_d^0 \rightarrow D^+ D^-, D^{*+} D^-, D^+ D^{*-})$, and they have quite complex variational trends to $|\lambda_{i23}^* \lambda_{i21}'|$ and $|\phi_{\text{RPV}}|$. The effects of $\lambda_{i23}^* \lambda_{i21}'$ couplings on $\mathcal{C}(B_d^0, \bar{B}_d^0 \rightarrow D^{*+} D^-)$ and $\mathcal{S}(B_d^0, \bar{B}_d^0 \rightarrow D^+ D^-, D^{*+} D^-)$ are shown in Fig. 3 (d-f). $\mathcal{C}(B_d^0, \bar{B}_d^0 \rightarrow D^+ D^{*-})$ has entirely different trends from $\mathcal{C}(B_d^0, \bar{B}_d^0 \rightarrow D^{*+} D^-)$. $\mathcal{S}(B_d^0, \bar{B}_d^0 \rightarrow D^+ D^{*-})$ has a similar trends as $\mathcal{S}(B_d^0, \bar{B}_d^0 \rightarrow D^{*+} D^-)$.

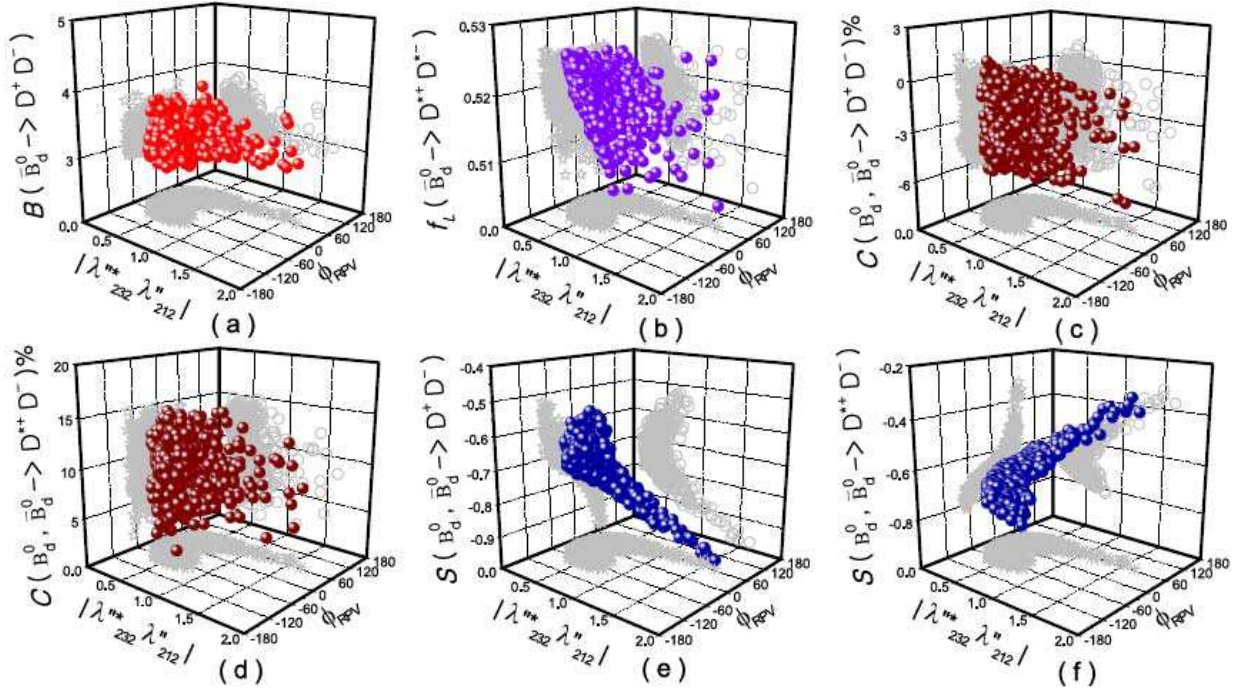


Figure 2: Effects of RPV coupling $\lambda_{232}^{*} \lambda_{212}^{*}$ in $\bar{B}_d^0 \rightarrow D^{(*)+} D^{(*)-}$ decays, where $|\lambda_{232}^{*} \lambda_{212}^{*}|$ is in units of 10^{-3} , and \mathcal{B} in units of 10^{-4} .

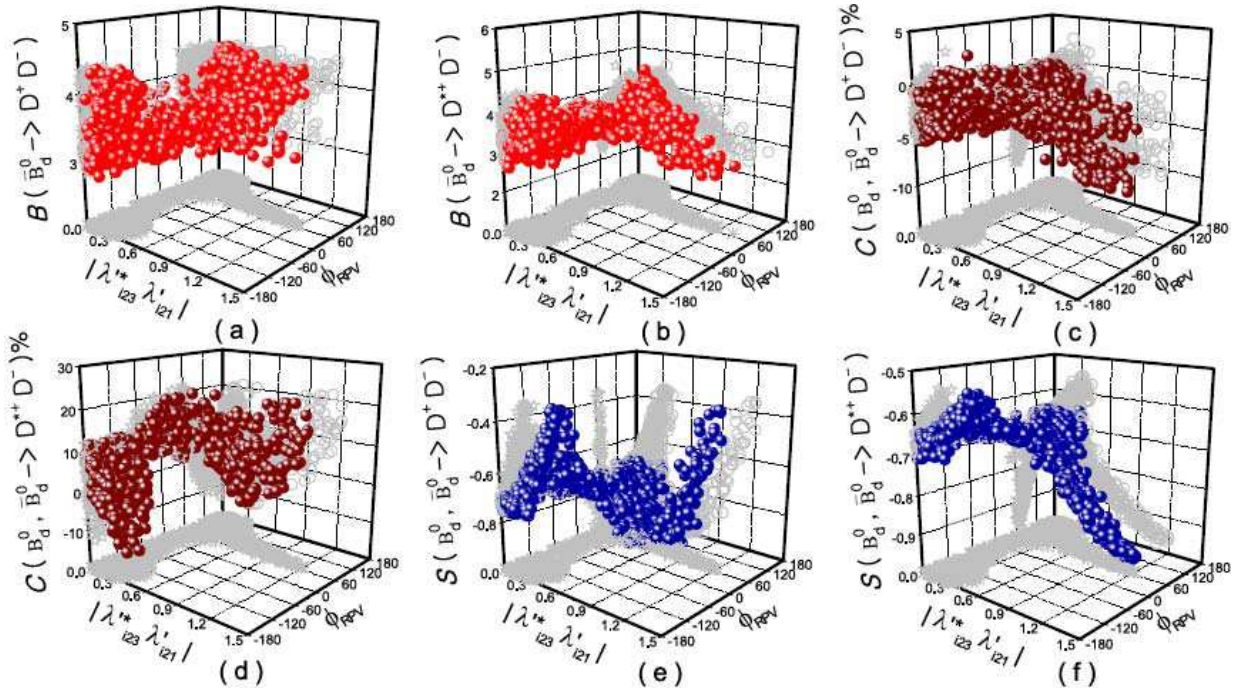


Figure 3: Effects of RPV coupling $\lambda_{i23}^{*} \lambda_{i21}^{*}$ in $\bar{B}_d^0 \rightarrow D^{(*)+} D^{(*)-}$ decays, where $|\lambda_{i23}^{*} \lambda_{i21}^{*}|$ is in units of 10^{-3} , and \mathcal{B} in units of 10^{-4} .

3.2 Exclusive color-allowed $b \rightarrow c\bar{c}s$ decays

Exclusive color-allowed $b \rightarrow c\bar{c}s$ tree decays include $\bar{B}_d^0 \rightarrow D^{(*)+} D_s^{(*)-}$, $B_u^- \rightarrow D^{(*)0} D_s^{(*)-}$ and $\bar{B}_s^0 \rightarrow D_s^{(*)+} D_s^{(*)-}$ decay modes. Almost all branching ratios and one longitudinal polarization have been measured by Belle [49], BABAR [27, 28, 29], CLEO [30, 31, 32, 33], and ARGUS [34] collaborations. Their averaged values from Particle Data Group [42] are listed as follows

$$\begin{aligned}
\mathcal{B}(\bar{B}_d^0 \rightarrow D^+ D_s^-) &= (7.4 \pm 0.7) \times 10^{-3}, & \mathcal{B}(\bar{B}_d^0 \rightarrow D^{*+} D_s^-) &= (8.3 \pm 1.1) \times 10^{-3}, \\
\mathcal{B}(\bar{B}_d^0 \rightarrow D^+ D_s^{*-}) &= (7.6 \pm 1.6) \times 10^{-3}, & \mathcal{B}(\bar{B}_d^0 \rightarrow D^{*+} D_s^{*-}) &= (17.9 \pm 1.4) \times 10^{-3}, \\
\mathcal{B}(B_u^- \rightarrow D^0 D_s^-) &= (10.3 \pm 1.7) \times 10^{-3}, & \mathcal{B}(B_u^- \rightarrow D^{*0} D_s^-) &= (8.4 \pm 1.7) \times 10^{-3}, \\
\mathcal{B}(B_u^- \rightarrow D^0 D_s^{*-}) &= (7.8 \pm 1.6) \times 10^{-3}, & \mathcal{B}(B_u^- \rightarrow D^{*0} D_s^{*-}) &= (17.5 \pm 2.3) \times 10^{-3}, \\
\mathcal{B}(\bar{B}_s^0 \rightarrow D_s^+ D_s^-) &= (11 \pm 4) \times 10^{-3}, & \mathcal{B}(\bar{B}_s^0 \rightarrow D_s^+ D_s^{*-}) &< 121 \times 10^{-3}, \\
\mathcal{B}(\bar{B}_s^0 \rightarrow D_s^{*+} D_s^{*-}) &< 257 \times 10^{-3}, & f_L(\bar{B}_d^0 \rightarrow D^{*+} D_s^{*-}) &= 0.52 \pm 0.05.
\end{aligned} \tag{33}$$

The SM predictions, in which the full theoretical uncertainties of input parameters are considered, are given in the second columns of Table 5 and Table 6. Theoretical predictions for the branching ratios and the polarization fractions are given in Table 5. Predicted CPAs are also given in Table 6. Compared with the experimental data, only the SM predictions of $\mathcal{B}(\bar{B}_d^0 \rightarrow D^{*+} D_s^{*-}, B_u^- \rightarrow D^{*0} D_s^{*-})$ are slightly larger than the corresponding experimental data given in Eq. (33), and all the other branching ratios are consistent with the data within 1σ error level. For the color-allowed $b \rightarrow c\bar{c}s$ decays the penguin effects are doubly Cabibbo-suppressed and, therefore, play a significantly less pronounced role in CPAs. These CPAs have not been measured yet. We obtain that all CPAs are expected to be very small (about 10^{-3} or 10^{-4} order) in the SM except $\mathcal{S}(B_s^0, \bar{B}_s^0 \rightarrow D_s^{*+} D_s^{*-})$ and $\mathcal{C}(B_s^0, \bar{B}_s^0 \rightarrow D_s^{*+} D_s^-, D_s^+ D_s^{*-})$. There is no obvious signature of CP violation in $B_s \rightarrow D_s^{*\pm} D_s^\mp$ decays since $\mathcal{C}(B_s^0, \bar{B}_s^0 \rightarrow D_s^{*+} D_s^-) \approx -\mathcal{C}(B_s^0, \bar{B}_s^0 \rightarrow D_s^+ D_s^{*-})$ and $\mathcal{S}(B_s^0, \bar{B}_s^0 \rightarrow D_s^{*+} D_s^-) \approx -\mathcal{S}(B_s^0, \bar{B}_s^0 \rightarrow D_s^+ D_s^{*-})$.

There are two RPV coupling products, $\lambda_{231}^{''*} \lambda_{221}^{''}$ and $\lambda_{i23}^{i*} \lambda_{i22}^{i'}$, contributing to these exclusive $b \rightarrow c\bar{c}s$ decay modes at tree level. We use the experimental data listed in Eq. (33) to constrain the RPV coupling products, and the allowed spaces are shown in Fig. 4. The coupling $\lambda_{231}^{''*} \lambda_{221}^{''}$ due to squark exchange contributes to all twelve relative decay modes. The allowed space of $\lambda_{231}^{''*} \lambda_{221}^{''}$ is shown in the left plot of Fig. 4. The slepton exchange couplings $\lambda_{i23}^{i*} \lambda_{i22}^{i'}$ contribute to six $\bar{B}_d^0 \rightarrow D^{(*)+} D_s^-, B_u^- \rightarrow D^{(*)0} D_s^-$ and $\bar{B}_s^0 \rightarrow D_s^{(*)+} D_s^-$ decays, and the constrained space is displayed in the right plot of Fig. 4. From Fig. 4, we find both moduli of RPV couplings have

Table 5: Theoretical predictions for CP averaged \mathcal{B} (in units of 10^{-4}) and polarization fractions (in units of 10^{-2}) of exclusive color-allowed $b \rightarrow c\bar{c}s$ decays in the SM and the RPV MSSM.

Observable	SM	MSSM w/ $\lambda_{231}^{\prime*} \lambda_{221}^{\prime\prime}$	MSSM w/ $\lambda_{i23}^{\prime*} \lambda_{i22}^{\prime}$
$\mathcal{B}(\bar{B}_d^0 \rightarrow D^+ D_s^-)$	[6.70, 10.65]	[6.38, 7.59]	[6.42, 8.80]
$\mathcal{B}(\bar{B}_d^0 \rightarrow D^{*+} D_s^-)$	[6.70, 10.45]	[6.47, 9.49]	[6.16, 9.30]
$\mathcal{B}(\bar{B}_d^0 \rightarrow D^+ D_s^{*-})$	[7.32, 13.22]	[6.90, 10.29]	
$\mathcal{B}(\bar{B}_d^0 \rightarrow D^{*+} D_s^{*-})$	[19.27, 34.42]	[18.59, 20.70]	
$\mathcal{B}(B_u^- \rightarrow D^0 D_s^-)$	[7.21, 11.43]	[6.90, 8.12]	[6.90, 9.49]
$\mathcal{B}(B_u^- \rightarrow D^{*0} D_s^-)$	[7.17, 11.24]	[6.95, 10.17]	[6.64, 9.96]
$\mathcal{B}(B_u^- \rightarrow D^0 D_s^{*-})$	[7.89, 14.27]	[7.43, 11.00]	
$\mathcal{B}(B_u^- \rightarrow D^{*0} D_s^{*-})$	[20.57, 37.06]	[19.99, 22.10]	
$\mathcal{B}(\bar{B}_s^0 \rightarrow D_s^+ D_s^-)$	[6.55, 10.72]	[6.36, 7.71]	[6.23, 9.05]
$\mathcal{B}(\bar{B}_s^0 \rightarrow D_s^{*+} D_s^-)$	[6.46, 10.44]	[6.51, 9.46]	[6.02, 9.26]
$\mathcal{B}(\bar{B}_s^0 \rightarrow D_s^+ D_s^{*-})$	[7.08, 12.97]	[7.00, 10.40]	
$\mathcal{B}(\bar{B}_s^0 \rightarrow D_s^{*+} D_s^{*-})$	[18.64, 33.83]	[18.48, 20.93]	
$f_L(\bar{B}_d^0 \rightarrow D^{*+} D_s^{*-})$	[50.25, 50.91]	[48.46, 51.13]	
$f_L(B_u^- \rightarrow D^{*0} D_s^{*-})$	[50.28, 50.94]	[48.49, 51.16]	
$f_L(\bar{B}_s^0 \rightarrow D_s^{*+} D_s^{*-})$	[50.40, 51.10]	[48.71, 51.30]	
$f_{\perp}(\bar{B}_d^0 \rightarrow D^{*+} D_s^{*-})$	[8.85, 9.55]	[8.15, 12.85]	
$f_{\perp}(B_u^- \rightarrow D^{*0} D_s^{*-})$	[8.87, 9.57]	[8.17, 12.88]	
$f_{\perp}(\bar{B}_s^0 \rightarrow D_s^{*+} D_s^{*-})$	[8.38, 9.07]	[7.71, 12.23]	

been limited as $|\lambda_{231}^{\prime*} \lambda_{221}^{\prime\prime}| < 8.05 \times 10^{-3}$ and $|\lambda_{i23}^{\prime*} \lambda_{i22}^{\prime}| < 5.05 \times 10^{-3}$. Their RPV weak phases are not constrained much when their magnitudes are less than about 1×10^{-3} .

Next, using the constrained parameter spaces shown in Fig. 4, we are going to predict RPV effects on the observables which have not been measured yet. We summarize RPV MSSM predictions with two separate RPV coupling contributions in the last two columns of Table 5 and Table 6.

The contributions of $\lambda_{231}^{\prime*} \lambda_{221}^{\prime\prime}$ coupling due to squark exchange are summarized in the third columns of Table 5 and Table 6. In Table 5, we find that the ranges of all branching ratios

Table 6: Theoretical predictions for CPAs (in units of 10^{-2}) of exclusive color-allowed $b \rightarrow c\bar{c}s$ decays in the SM and the RPV MSSM.

Observable	SM	MSSM w/ $\lambda''_{231} \lambda''_{221}$	MSSM w/ $\lambda'_{i23} \lambda'_{i22}$
$\mathcal{A}_{\text{CP}}^{\text{dir}}(\bar{B}_d^0 \rightarrow D^+ D_s^-)$	$[-0.34, -0.22]$	$[-3.06, 2.58]$	$[-8.42, 7.94]$
$\mathcal{A}_{\text{CP}}^{\text{dir}}(\bar{B}_d^0 \rightarrow D^{*+} D_s^-)$	$[0.03, 0.06]$	$[-0.32, 0.36]$	$[-0.98, 1.07]$
$\mathcal{A}_{\text{CP}}^{\text{dir}}(\bar{B}_d^0 \rightarrow D^+ D_s^{*-})$	$[-0.07, -0.06]$	$[-0.51, 0.44]$	
$\mathcal{A}_{\text{CP}}^{+, \text{dir}}(\bar{B}_d^0 \rightarrow D^{*+} D_s^{*-})$	$[-0.07, -0.06]$	$[-0.69, 0.56]$	
$\mathcal{A}_{\text{CP}}^{\text{dir}}(B_u^- \rightarrow D^0 D_s^-)$	$[-0.34, -0.22]$	$[-3.06, 2.58]$	$[-8.42, 7.94]$
$\mathcal{A}_{\text{CP}}^{\text{dir}}(B_u^- \rightarrow D^{*0} D_s^-)$	$[0.03, 0.06]$	$[-0.32, 0.36]$	$[-0.98, 1.07]$
$\mathcal{A}_{\text{CP}}^{\text{dir}}(B_u^- \rightarrow D^0 D_s^{*-})$	$[-0.07, -0.06]$	$[-0.51, 0.58]$	
$\mathcal{A}_{\text{CP}}^{+, \text{dir}}(B_u^- \rightarrow D^{*0} D_s^{*-})$	$[-0.07, -0.06]$	$[-0.69, 0.56]$	
$\mathcal{S}(B_s^0, \bar{B}_s^0 \rightarrow D_s^+ D_s^-)$	$[0.40, 0.61]$	$[-59.67, 61.80]$	$[-99.84, 99.79]$
$\mathcal{S}(B_s^0, \bar{B}_s^0 \rightarrow D_s^{*+} D_s^-)$	$[1.33, 2.16]$	$[-46.48, 47.65]$	$[-56.04, 59.14]$
$\mathcal{S}(B_s^0, \bar{B}_s^0 \rightarrow D_s^+ D_s^{*-})$	$[-2.20, -1.31]$	$[-49.26, 45.22]$	$[-58.96, 56.60]$
$\mathcal{S}^+(B_s^0, \bar{B}_s^0 \rightarrow D_s^{*+} D_s^{*-})$	$[-31.81, -29.15]$	$[-54.41, 55.49]$	
$\mathcal{C}(B_s^0, \bar{B}_s^0 \rightarrow D_s^+ D_s^-)$	$[0.22, 0.34]$	$[-2.58, 3.06]$	$[-7.94, 8.42]$
$\mathcal{C}(B_s^0, \bar{B}_s^0 \rightarrow D_s^{*+} D_s^-)$	$[2.77, 13.39]$	$[3.15, 10.13]$	$[0.79, 28.22]$
$\mathcal{C}(B_s^0, \bar{B}_s^0 \rightarrow D_s^+ D_s^{*-})$	$[-13.36, -2.76]$	$[-10.08, -3.14]$	$[-29.14, -0.54]$
$\mathcal{C}^+(B_s^0, \bar{B}_s^0 \rightarrow D_s^{*+} D_s^{*-})$	$[0.06, 0.07]$	$[-0.56, 0.69]$	

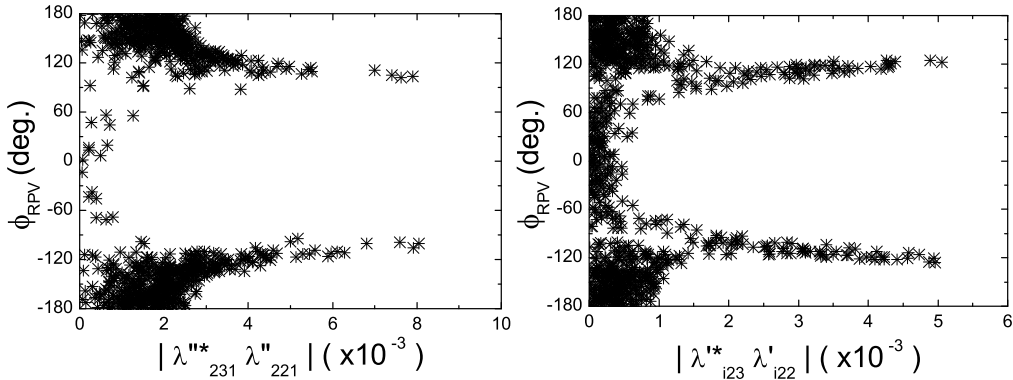


Figure 4: Allowed parameter spaces for relevant RPV coupling products constrained by the measurements of exclusive color-allowed $b \rightarrow c\bar{c}s$ decays listed in Eq. (33).

are shrunk by $\lambda''_{231} \lambda''_{221}$ coupling and the experimental constraints. Especially, $\lambda''_{231} \lambda''_{221}$ coupling effects could reduce the range of $\mathcal{B}(\bar{B}_s^0 \rightarrow D_s^{*+} D_s^{*-})$. However, the allowed ranges of three $f_L(B_{(s)} \rightarrow D_{(s)}^* D_s^*)$ and three $f_\perp(B_{(s)} \rightarrow D_{(s)}^* D_s^*)$ are enlarged by $\lambda''_{231} \lambda''_{221}$ coupling. In Table 6, we can see $\lambda''_{231} \lambda''_{221}$ coupling does not affect $\mathcal{C}(\bar{B}_s^0 \rightarrow D_s^{*+} D_s^-, D_s^{*+} D_s^-)$ much.

Meanwhile, RPV coupling effects could remarkably enlarge the allowed ranges of the other direct CPAs (about 10 times). Unfortunately, they are still too small to be measured at presently available experiments. It is interesting to note that mixing-induced CPAs of B_s decays are greatly affected by $\lambda''_{231} \lambda''_{221}$ coupling. For an example, $|\mathcal{S}(\bar{B}_s^0 \rightarrow D_s^{(*)+} D_s^{(*)-})|$ could be increased to $\sim 50\%$ and their signs could be changed by the squark exchange coupling.

The contributions of $\lambda'_{i23} \lambda'_{i22}$ due to the slepton exchanges are listed in the last columns of Table 5 and Table 6. From Table 5, we find the ranges of all branching ratios are shrunk by $\lambda'_{i23} \lambda'_{i22}$ coupling and the experimental constraints. The last columns of Table 6 show that $\lambda'_{i23} \lambda'_{i22}$ coupling could enlarge the ranges of all the CPAs. Particularly, $\lambda'_{i23} \lambda'_{i22}$ coupling could change the predicted $\mathcal{S}(B_s^0, \bar{B}_s^0 \rightarrow D_s^{(*)} D_s)$ significantly from quite narrow SM ranges to $[-0.6, 0.6]$ or $[-1, 1]$. The upper limits of $|\mathcal{C}(B_s^0, \bar{B}_s^0 \rightarrow D_s^{*+} D_s^-, D_s^+ D_s^{*-})|$ are increased a lot by $\lambda'_{i23} \lambda'_{i22}$ couplings.

Since RPV contributions to physical observables are also very similar in $\bar{B}_d^0 \rightarrow D^{(*)+} D_s^{(*)-}$, $B_u^- \rightarrow D^{(*)0} D_s^{(*)-}$ and $\bar{B}_s^0 \rightarrow D_s^{(*)+} D_s^{(*)-}$ systems, we show only a few observables of B_s decays as examples. Fig. 5 and Fig. 6 show the variational trends in some observables with the $\lambda''_{231} \lambda''_{221}$ and $\lambda'_{i23} \lambda'_{i22}$ couplings, respectively.

First, we will elucidate the information implied in Fig. 5. From Fig. 5 (a), we find $\mathcal{B}(\bar{B}_s^0 \rightarrow D_s^{*+} D_s^{*-})$ is not changed much by $|\lambda''_{231} \lambda''_{221}|$, and could have only small value when ϕ_{RPV} is not too large. As shown in Fig. 5(b), $f_\perp(\bar{B}_s^0 \rightarrow D_s^{*+} D_s^{*-})$ is increasing with $|\lambda''_{231} \lambda''_{221}|$ and also could have small value when ϕ_{RPV} is small. From Fig. 5 (c-d), we find $|\mathcal{S}(B_s^0, \bar{B}_s^0 \rightarrow D_s^+ D_s^-, D_s^{*+} D_s^-)|$ are all rapidly increasing with $|\lambda''_{231} \lambda''_{221}|$ and could be very large at the large values of $|\lambda''_{231} \lambda''_{221}|$ and $|\phi_{\text{RPV}}|$, furthermore, the RPV weak phase has opposite effects between $|\mathcal{S}(B_s^0, \bar{B}_s^0 \rightarrow D_s^+ D_s^-)|$ and $|\mathcal{S}(B_s^0, \bar{B}_s^0 \rightarrow D_s^{*+} D_s^-)|$. $\lambda''_{231} \lambda''_{221}$ coupling effects on $\mathcal{S}(B_s^0, \bar{B}_s^0 \rightarrow D_s^+ D_s^{*-})$ ($\mathcal{S}(B_s^0, \bar{B}_s^0 \rightarrow D_s^{*+} D_s^{*-})$) are similar as ones on $\mathcal{S}(B_s^0, \bar{B}_s^0 \rightarrow D_s^{*+} D_s^-)$ ($\mathcal{S}(B_s^0, \bar{B}_s^0 \rightarrow D_s^+ D_s^-)$). So any measurement of $\mathcal{S}(B_s^0, \bar{B}_s^0 \rightarrow D_s^{(*)+} D_s^{(*)-})$ in the future will strongly constrain the magnitude and RPV weak phase of $\lambda''_{231} \lambda''_{221}$ coupling, and then other mixing-induced CPAs will be more accurately predicted as indicated by Fig. 5 (c-d). As shown in Fig. 5 (e), $\mathcal{C}(B_s^0, \bar{B}_s^0 \rightarrow D_s^+ D_s^-)$ has similar trends as $\mathcal{S}(B_s^0, \bar{B}_s^0 \rightarrow D_s^+ D_s^-)$ with $|\lambda''_{231} \lambda''_{221}|$ and ϕ_{RPV} ,

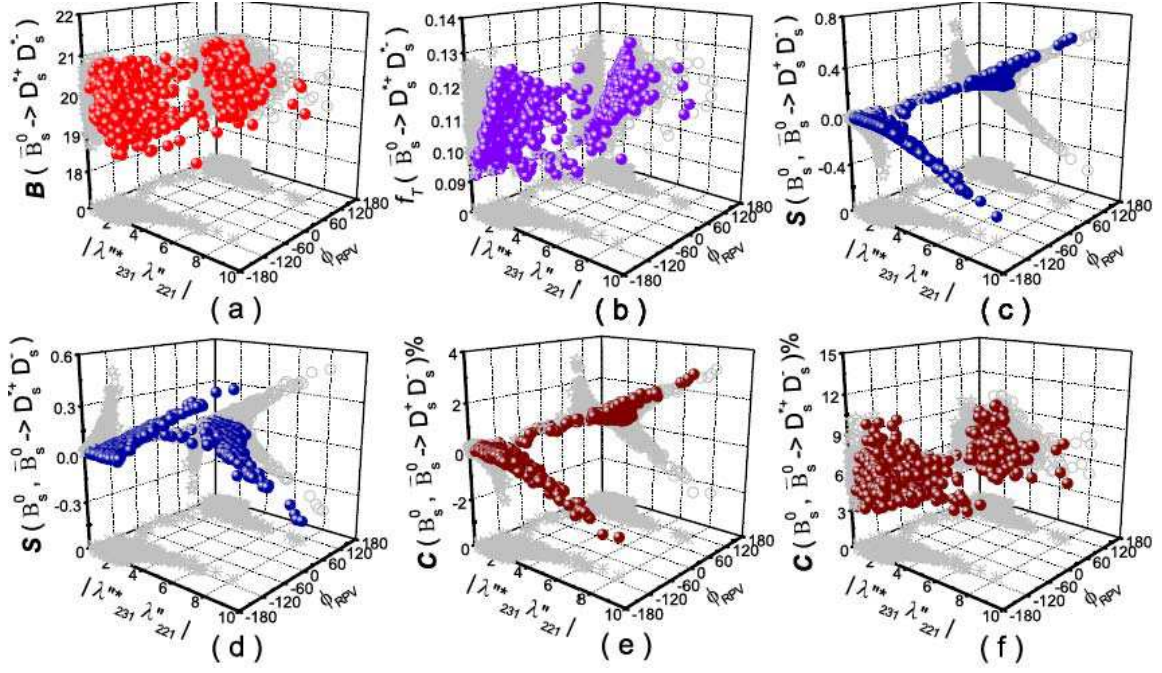


Figure 5: Effects of RPV coupling $\lambda_{231}^{\prime*} \lambda_{221}^{\prime}$ in $\bar{B}_s^0 \rightarrow D_s^{(*)+} D_s^{(*)-}$ decays, where $|\lambda_{231}^{\prime*} \lambda_{221}^{\prime}|$ is in units of 10^{-3} , \mathcal{B} in units of 10^{-4} , and f_T denotes the transverse polarization fraction f_{\perp} .

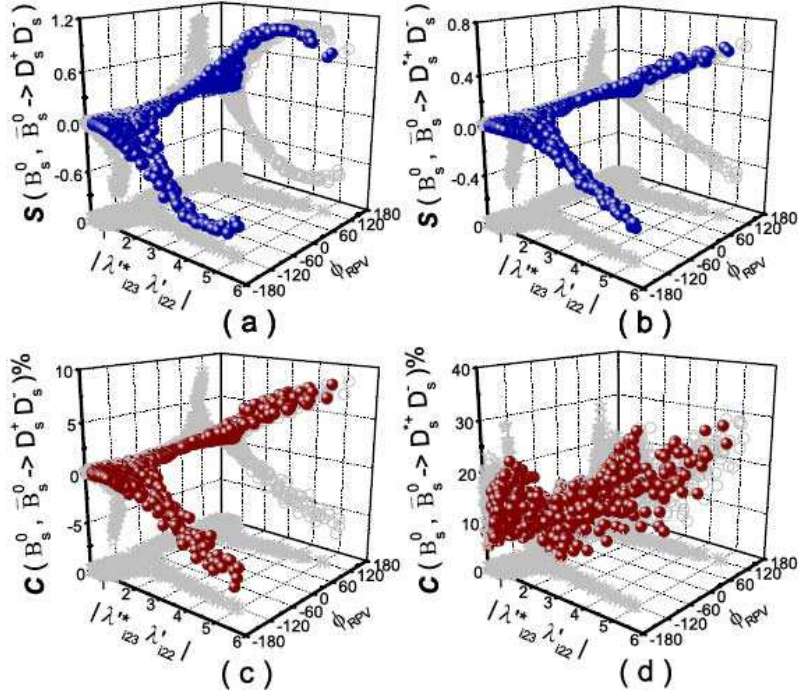


Figure 6: Effects of $\lambda_{i23}^{\prime*} \lambda_{i22}^{\prime}$ in $\bar{B}_s^0 \rightarrow D_s^{(*)+} D_s^{(*)-}$ decays, where $|\lambda_{i23}^{\prime*} \lambda_{i22}^{\prime}|$ are in units of 10^{-3} , and \mathcal{B} in units of 10^{-4} .

however, $\lambda_{231}''^* \lambda_{221}''$ coupling effects on the former are much smaller than the effects on the latter. $\mathcal{A}_{\text{CP}}^{\text{dir}}(B_{u,d} \rightarrow DD_s^-, D^* D_s^-, D^* D_s^{*-})$ and $-\mathcal{A}_{\text{CP}}^{\text{dir}}(B_{u,d} \rightarrow DD_s^{*-})$ have the same variational trends with $\lambda_{231}''^* \lambda_{221}''$ as $\mathcal{C}(B_s^0, \bar{B}_s^0 \rightarrow D_s^+ D_s^-)$ has. $\mathcal{C}(B_s^0, \bar{B}_s^0 \rightarrow D_s^{*+} D_s^-, D_s^{*+} D_s^-)$ are not affected much by $\lambda_{231}''^* \lambda_{221}''$ coupling, and we show $\mathcal{C}(B_s^0, \bar{B}_s^0 \rightarrow D_s^{*+} D_s^-)$ in Fig. 5 (f) as an example.

Fig. 6 illustrates $\lambda_{i23}^* \lambda'_{i22}$ contributions to the CPAs of $\bar{B}_s^0 \rightarrow D_s^{(*)+} D_s^-$. As displayed in Fig. 6 (a-b), $\mathcal{S}(B_s^0, \bar{B}_s^0 \rightarrow D_s^{(*)+} D_s^-)$ are very sensitive to $\lambda_{i23}^* \lambda'_{i22}$ couplings. $|\mathcal{S}(B_s^0, \bar{B}_s^0 \rightarrow D_s^{(*)+} D_s^-)|$ are strongly increasing with $|\lambda_{i23}^* \lambda'_{i22}|$, and they could reach extremum at $|\phi_{\text{RPV}}| \approx 120^\circ$. The $\lambda_{i23}^* \lambda'_{i22}$ coupling effects on $\mathcal{S}(B_s^0, \bar{B}_s^0 \rightarrow D_s^+ D_s^{*-})$ are same as the ones on $\mathcal{S}(B_s^0, \bar{B}_s^0 \rightarrow D_s^{*+} D_s^-)$. Fig. 6 (c) shows that $\mathcal{C}(B_s^0, \bar{B}_s^0 \rightarrow D_s^+ D_s^-)$ are also very sensitive to $|\lambda_{i23}^* \lambda'_{i22}|$ and ϕ_{RPV} , but it is still too small to be measured in near future. In addition, $\mathcal{A}_{\text{CP}}^{\text{dir}}(B_{u,d} \rightarrow D^{(*)} D_s^-)$ are affected much by $\lambda_{i23}^* \lambda'_{i22}$ couplings, and just RPV MSSM predictions of these quantities are very small. $\lambda_{i23}^* \lambda'_{i22}$ couplings could have similar impacts on $\mathcal{C}(B_s^0, \bar{B}_s^0 \rightarrow D_s^{*+} D_s^-)$ and $-\mathcal{C}(B_s^0, \bar{B}_s^0 \rightarrow D_s^{*+} D_s^-)$. We give these coupling effects on $\mathcal{C}(B_s^0, \bar{B}_s^0 \rightarrow D_s^{*+} D_s^-)$ in Fig. 6 (d), which shows $\mathcal{C}(B_s^0, \bar{B}_s^0 \rightarrow D_s^{*+} D_s^-)$ is increasing with $|\lambda_{i23}^* \lambda'_{i22}|$, and could have large value at large $|\phi_{\text{RPV}}|$.

4 Summary

We have studied the twenty-four double charm decays $\bar{B}_d^0 \rightarrow D^{(*)+} D_{(s)}^{(*)-}$, $B_u^- \rightarrow D^{(*)0} D_{(s)}^{(*)-}$ and $\bar{B}_s^0 \rightarrow D_s^{(*)+} D_{(s)}^{(*)-}$ in the RPV MSSM. We have treated these decays in the naive factorization and removed the known k^2 ambiguities in the penguin contributions via $b \rightarrow qg^*(\gamma^*) \rightarrow qc\bar{c}$ by calculating its hard kernel $b \rightarrow c + D_q$. Considering the theoretical uncertainties and the experimental error-bars, we have obtained fairly constrained parameter spaces of RPV couplings from the present experimental data, which have quite highly consistent measurements among the relative collaborations. Furthermore, using the constrained RPV coupling parameter spaces, we have predicted the RPV effects on the branching ratios, the CPAs and the polarization fractions, which have not been measured or have not been well measured yet.

The investigation of exclusive color-allowed $b \rightarrow c\bar{c}d$ decays is motivated by the large direct CPA $\mathcal{C}(B_d^0, \bar{B}_d^0 \rightarrow D^+ D^-)$ reported by Belle, which has not been confirmed by BABAR yet and contradicted the SM prediction. Using the most conservative experimental bounds from $\bar{B}_d^0 \rightarrow D^{(*)+} D^{(*)-}$ and $B_u^- \rightarrow D^{(*)0} D^{(*)-}$ systems (choose only twelve highly consistent measurements between BABAR and Belle), we have first obtained quite strong constraints on the involved

RPV couplings $\lambda''_{232}\lambda''_{212}$ and $\lambda'_{i23}\lambda'_{i21}$ from $b \rightarrow c\bar{c}d$ transition, due to squark exchange and slepton exchanges, respectively. Then, using the constrained RPV coupling parameter spaces, we have predicted the RPV effects on $\mathcal{C}(B_d^0, \bar{B}_d^0 \rightarrow D^+D^-)$ and other observables, which have less consistent measurements or have not been measured yet. We have found that the lower limit of $\mathcal{C}(B_d^0, \bar{B}_d^0 \rightarrow D^{(*)+}D^-)$ could be slightly reduced by the RPV couplings. Our RPV MSSM prediction of $\mathcal{C}(B_d^0, \bar{B}_d^0 \rightarrow D^+D^-)$ is consistent with BABAR measurement within 1σ error level, but cannot explain the corresponding Belle experimental data within 3σ level. We have also found that the contributions of $\lambda''_{232}\lambda''_{212}$ and $\lambda'_{i23}\lambda'_{i21}$ cannot affect the relevant branching ratios much. $\lambda''_{232}\lambda''_{212}$ or $\lambda'_{i23}\lambda'_{i21}$ contributions could greatly enlarge the ranges of the relevant mixing-induced CPAs $\mathcal{S}(B_d^0, \bar{B}_d^0 \rightarrow D^{(*)+}D^{(*)-})$ from their SM predictions, and these quantities are very sensitive to the moduli and weak phases of $\lambda''_{232}\lambda''_{212}$ and $\lambda'_{i23}\lambda'_{i21}$. So more accurate measurements of $\mathcal{S}(B_d^0, \bar{B}_d^0 \rightarrow D^{(*)+}D^{(*)-})$ in the future will much more strongly constrain these RPV couplings, and then mixing-induced CPAs can be more accurately predicted as well. Effects of $\lambda''_{232}\lambda''_{212}$ coupling could slightly extend the allowed regions of four $\mathcal{C}(B_d^0, \bar{B}_d^0 \rightarrow D^{(*)+}D^{(*)-})$ and eight $\mathcal{A}_{\text{CP}}^{\text{dir}}(B_u^- \rightarrow D^{(*)0}D^{(*)-}, \bar{B}_s^0 \rightarrow D_s^{(*)+}D_s^{(*)-})$. $\mathcal{C}(B_d^0, \bar{B}_d^0 \rightarrow D^{(*)+}D^-)$ are also sensitive to the slepton exchange couplings $\lambda'_{i23}\lambda'_{i21}$, and their signs could be changed by these couplings. Additionally, three $f_L(B_{(s)} \rightarrow D_{(s)}^*D^*)$ and three $f_{\perp}(B_{(s)} \rightarrow D_{(s)}^*D^*)$ are decreased and increased by $\lambda''_{232}\lambda''_{212}$ coupling, respectively, and their allowed ranges are magnified by these couplings.

For $\bar{B}_d^0 \rightarrow D^{(*)+}D_s^{(*)-}$, $B_u^- \rightarrow D^{(*)0}D_s^{(*)-}$ and $\bar{B}_s^0 \rightarrow D_s^{(*)+}D_s^{(*)-}$ decays, RPV couplings $\lambda'_{231}\lambda''_{221}$ and $\lambda'_{i23}\lambda'_{i22}$ contribute to these decay modes. We have found $\lambda''_{231}\lambda''_{221}$ coupling effects could apparently suppress the upper limit of $\mathcal{B}(\bar{B}_s^0 \rightarrow D_s^{*+}D_s^{*-})$, and could slightly enlarge the allowed ranges of three $f_L(B_{(s)} \rightarrow D_{(s)}^*D_s^*)$ and three $f_{\perp}(B_{(s)} \rightarrow D_{(s)}^*D_s^*)$, nevertheless these quantities are not very sensitive to the changes of $|\lambda''_{231}\lambda''_{221}|$ and ϕ_{RPV} . $\mathcal{C}(\bar{B}_s^0 \rightarrow D_s^{*+}D_s^-, D_s^+D_s^{*-})$ are not evidently affected by the squark exchange $\lambda''_{231}\lambda''_{221}$ coupling, and their upper limits are increased a lot by the slepton exchange $\lambda'_{i23}\lambda'_{i22}$ couplings. RPV couplings $\lambda''_{231}\lambda''_{221}$ and $\lambda'_{i23}\lambda'_{i22}$ could greatly enlarge all other CP asymmetries, which are also very sensitive to the relevant RPV couplings. However, the direct CPAs are still too small to be measured soon. We could explore RPV MSSM effects from the mixing-induced CPAs of B_s decays.

With the large amount of B decay data from BABAR and Belle, especially from LHCb in the near future, measurements of previously known observables will become more precise and many unobserved observables will be also measured. From the comparison of our predictions

in Figs. 2-3 and Figs 5-6 with near future experiments, one will obtain more stringent bounds on the product combinations of the RPV couplings. On the other hand, the RPV MSSM predictions of other decays will become more precise by the more stringent bounds on the RPV couplings. The results in this paper could be useful for probing RPV MSSM effects, and will correlate with searches for direct supersymmetry signals at future experiments, for example, the LHC.

Acknowledgments

The work of C.S. Kim was supported in part by CHEP-SRC and in part by the KRF Grant funded by the Korean Government (MOEHRD) No. KRF-2005-070-C00030. The work of Ru-Min Wang was supported by the second stage of Brain Korea 21 Project. The work of Ya-Dong Yang was supported by the National Science Foundation under contract Nos. 10675039 and 10735080.

References

- [1] A. I. Sanda and Z. z. Xing, Phys. Rev. D **56**, 341 (1997) [arXiv:hep-ph/9702297].
- [2] Z. z. Xing, Phys. Rev. D **61**, 014010 (1999) [arXiv:hep-ph/9907455], and references therein.
- [3] S. Fratina *et al.*, Phys. Rev. Lett. **98**, 221802 (2007) [arXiv:hep-ex/0702031].
- [4] J. Anderson *et al.* [BABAR Collaboration], arXiv:0808.1866 [hep-ex].
- [5] T. Aushev *et al.* [Belle Collaboration], Phys. Rev. Lett. **93**, 201802 (2004) [arXiv:hep-ex/0408051].
- [6] B. Aubert *et al.* [BABAR Collaboration], Phys. Rev. D **76**, 111102 (2007) [arXiv:0708.1549 [hep-ex]].
- [7] H. Miyake *et al.* [Belle Collaboration], Phys. Lett. B **618**, 34 (2005) [arXiv:hep-ex/0501037].
- [8] K. Vervink, arXiv:0810.3167 [hep-ex].

- [9] B. Aubert *et al.* [BABAR Collaboration], Phys. Rev. D **73**, 112004 (2006) [arXiv:hep-ex/0604037].
- [10] K. Abe *et al.* [Belle Collaboration], [arXiv:0708.1668 [hep-ex]].
- [11] G. Majumder *et al.* [Belle Collaboration], Phys. Rev. Lett. **95** (2005) 041803.
- [12] R. Zwicky, Phys. Rev. D **77**, 036004 (2008) [arXiv:0707.0677 [hep-ph]].
- [13] R. Fleischer, Eur. Phys. J. C **51**, 849 (2007) [arXiv:0705.4421 [hep-ph]].
- [14] M. Gronau, J. L. Rosner and D. Pirjol, Phys. Rev. D **78**, 033011 (2008).
- [15] P. Fayet, Nucl. Phys. B **90**, 104 (1975); Phys. Lett. B **64**, 159 (1976); Phys. Lett. B **69**, 489 (1977); Phys. Lett. B **84**, 416 (1979).
- [16] K. Inoue, A. Komatsu and S. Takeshita, Prog. Theor. Phys. **68**, 927 (1982); (E) *ibid.* **70**, 330 (1983); H. Nilles, Phys. Rept. **110**, 1 (1984); H. Haber and G. Kane, Phys. Rept. **117**, 75 (1985).
- [17] S. Weinberg, Phys. Rev. D **26**, 287 (1982).
- [18] N. Sakai and T. Yanagida, Nucl. Phys. B **197**, 533 (1982); C. Aulakh and R. Mohapatra, Phys. Lett. B **119**, 136 (1982).
- [19] See, for example, R. Barbier *et al.*, hep-ph/9810232, Phys. Rept. **420**, 1 (2005), and references therein; M. Chemtob, Prog. Part. Nucl. Phys. **54**, 71 (2005).
- [20] B. C. Allanach *et al.*, hep-ph/9906224, and references therein.
- [21] G. Bhattacharyya and A. Datta, Phys. Rev. Lett. **83**, 2300 (1999) [arXiv:hep-ph/9903490]; G. Bhattacharyya and A. Raychaudhuri, Phys. Rev. D **57**, R3837 (1998) [arXiv:hep-ph/9712245]; R. Wang, G. R. Lu, E. K. Wang and Y. D. Yang, Eur. Phys. J. C **47**, 815 (2006) [arXiv:hep-ph/0603088].
- [22] A. Datta, Phys. Rev. D **66**, 071702 (2002) [arXiv:hep-ph/0208016]; D. Chakraverty and D. Choudhury, Phys. Rev. D **63**, 075009 (2001) [arXiv:hep-ph/0008165]; B. Dutta, C. S. Kim and S. Oh, Phys. Lett. B **535**, 249 (2002) [arXiv:hep-ph/0202019]; B. Dutta, C. S. Kim and S. Oh, Phys. Rev. Lett. **90**, 011801 (2003) [arXiv:hep-ph/0208226].

- [23] S. Nandi and J. P. Saha, Phys. Rev. D **74**, 095007 (2006) [arXiv:hep-ph/0608341]; Y. G. Xu, R. M. Wang and Y. D. Yang, Phys. Rev. D **74**, 114019 (2006) [arXiv:hep-ph/0610338]; C. S. Kim and R. M. Wang, Phys. Rev. D **77**, 094006 (2008) [arXiv:0712.2954 [hep-ph]]; J. P. Saha and A. Kundu, Phys. Rev. D **66**, 054021 (2002) [arXiv:hep-ph/0205046].
- [24] B. Dutta, C. S. Kim, S. Oh and G. h. Zhu, Eur. Phys. J. C **37**, 273 (2004) [arXiv:hep-ph/0312388]; B. Dutta, C. S. Kim, S. Oh and G. h. Zhu, Phys. Lett. B **601**, 144 (2004) [arXiv:hep-ph/0312389]; Y. D. Yang, R. M. Wang and G. R. Lu, Phys. Rev. D **72**, 015009 (2005) [arXiv:hep-ph/0411211].
- [25] M. Wirbel, B. Stech and M. Bauer, Z. Phys. C **29**, 637 (1985); M. Bauer, B. Stech and M. Wirbel, Z. Phys. C **34**, 103 (1987).
- [26] K. Abe *et al.* [Belle Collaboration], Phys. Rev. Lett. **89**, 122001 (2002) [arXiv:hep-ex/0206014].
- [27] B. Aubert *et al.* [BABAR Collaboration], Phys. Rev. D **67**, 092003 (2003) [arXiv:hep-ex/0302015].
- [28] B. Aubert *et al.* [BABAR Collaboration], Phys. Rev. D **74**, 031103 (2006) [arXiv:hep-ex/0605036].
- [29] B. Aubert *et al.* [BABAR Collaboration], Phys. Rev. D **71**, 091104 (2005) [arXiv:hep-ex/0502041].
- [30] S. Ahmed *et al.* [CLEO Collaboration], Phys. Rev. D **62**, 112003 (2000) [arXiv:hep-ex/0008015].
- [31] D. Gibaut *et al.* [CLEO Collaboration], Phys. Rev. D **53**, 4734 (1996).
- [32] D. Bortoletto *et al.* [CLEO Collaboration], Phys. Rev. D **45**, 21 (1992).
- [33] D. Bortoletto *et al.*, Phys. Rev. Lett. **64**, 2117 (1990).
- [34] H. Albrecht *et al.* [ARGUS Collaboration], Z. Phys. C **54**, 1 (1992).
- [35] G. Buchalla, A. J. Buras and M. E. Lautenbacher, Rev. Mod. Phys. **68**, 1125 (1996) [arXiv:hep-ph/9512380].

- [36] M. Wirbel, B. Stech and M. Bauer, Z. Phys. C **29**, 637 (1985).
- [37] M. Neubert and V. Rieckert, Nucl. Phys. B **382**, 97 (1992).
- [38] M. Gronau, Phys. Lett. B **233**, 479 (1989).
- [39] J. Soto, Nucl. Phys. B **316**, 141 (1989).
- [40] W. F. Palmer and Y. L. Wu, Phys. Lett. B **350**, 245 (1995) [arXiv:hep-ph/9501295].
- [41] A. Ali, G. Kramer and C. D. Lu, Phys. Rev. D **59**, 014005 (1998) [arXiv:hep-ph/9805403].
- [42] W.-M. Yao et al., Journal of Physics, G **33**, 1 (2006) and 2007 partial update for 2008, <http://pdg.lbl.gov/>.
- [43] J. Charles et al. (CKMfitter Group), Eur. Phys. J. C **41**, 1 (2005) [arXiv:hep-ph/0406184], updated results and plots available at: <http://ckmfitter.in2p3.fr/>.
- [44] C. Aubin *et al.*, Phys. Rev. Lett. **95**, 122002 (2005) [arXiv:hep-lat/0506030].
- [45] M. Neubert, Phys. Rept. **245**, 259 (1994) [arXiv:hep-ph/9306320].
- [46] M. Neubert, Int. J. Mod. Phys. A **11**, 4173 (1996) [arXiv:hep-ph/9604412].
- [47] M. Neubert, Phys. Rev. D **46**, 2212 (1992).
- [48] H. Y. Cheng, C. K. Chua and C. W. Hwang, Phys. Rev. D **69**, 074025 (2004) [arXiv:hep-ph/0310359].
- [49] A. Zupanc *et al.*, Phys. Rev. D **75**, 091102 (2007) [arXiv:hep-ex/0703040].